AMERICAN SOCIETY FOR MICROBIOLOGY | Antimicrobial Agents and Chemotherapy

Metabolomic Profiling of the Malaria Box Reveals Antimalarial Target Pathways

Erik L. Allman,[a] Heather J. Painter,[a] Jasmeet Samra,[a] Manuela Carrasquilla,[a]* Manuel Llinás[a,b]

Department of Biochemistry & Molecular Biology and Huck Center for Malaria Research, Pennsylvania State University, University Park, Pennsylvania, USA[a]; Department of Chemistry, Pennsylvania State University, University Park, Pennsylvania, USA[b]

The threat of widespread drug resistance to frontline antimalarials has renewed the urgency for identifying inexpensive chemotherapeutic compounds that are effective against *Plasmodium falciparum*, the parasite species responsible for the greatest number of malaria-related deaths worldwide. To aid in the fight against malaria, a recent extensive screening campaign has generated thousands of lead compounds with low micromolar activity against blood stage parasites. A subset of these leads has been compiled by the Medicines for Malaria Venture (MMV) into a collection of structurally diverse compounds known as the MMV Malaria Box. Currently, little is known regarding the activity of these Malaria Box compounds on parasite metabolism during intraerythrocytic development, and a majority of the targets for these drugs have yet to be defined. Here we interrogated the *in vitro* metabolic effects of 189 drugs (including 169 of the drug-like compounds from the Malaria Box) using ultra-high-performance liquid chromatography–mass spectrometry (UHPLC-MS). The resulting metabolic fingerprints provide information on the parasite biochemical pathways affected by pharmacologic intervention and offer a critical blueprint for selecting and advancing lead compounds as next-generation antimalarial drugs. Our results reveal several major classes of metabolic disruption, which allow us to predict the mode of action (MoA) for many of the Malaria Box compounds. We anticipate that future combination therapies will be greatly informed by these results, allowing for the selection of appropriate drug combinations that simultaneously target multiple metabolic pathways, with the aim of eliminating malaria and forestalling the expansion of drug-resistant parasites in the field.

Infection by the human malaria parasite *Plasmodium falciparum* rapidly leads to the clinical symptoms associated with the 48-h asexual replicative cycle of the parasite within the blood of the host, ultimately resulting in massive anemia and complications due to blood vessel occlusion (1). *P. falciparum* malaria continues to present an enormous global public health burden due to the lack of an effective long-term vaccine (2) and the emergence of resistance to frontline antimalarial chemotherapies (3). This underscores the continued need to maintain a robust drug development pipeline that produces novel and effective antimalarial compounds for future deployment. To catalyze drug discovery efforts, the Medicines for Malaria Venture (MMV) released an open-access "Malaria Box" that contains 200 drug-like and 200 probe-like compounds (4) which were found to be active and potent against blood stage *P. falciparum* (5–7). The freely available Malaria Box (http://www.mmv.org/research-development/open-access-malaria-box) has spawned an open-source, collaborative international effort to determine compound mode of action (MoA) in order to facilitate lead optimization (8).

Currently, the Malaria Box has been screened against a number of *P. falciparum* targets and multiple developmental stages (9–19), as well as other pathogens (20–29). These studies have identified compounds in the Malaria Box with efficacy against specific metabolic processes, such as the thioredoxin system (9), isoprenoid biosynthesis (14, 30), and aminopeptidases (11), as well as protein translation (10) and beta-hematin formation (17). A large group of related studies has also tested the Malaria Box on the sexual stages, using a wide variety of assays (12–16, 31–34). However, the use of phenotypic or endpoint-based assays in many of these profiling studies has produced varied results, providing limited insight toward identifying the targets of these compounds. On the other hand, the analysis of drug-resistant parasite lines generated in the laboratory (35–43) or of drug-resistant field isolates (44, 45) has provided information on the mechanism(s) of resistance and some molecular insights into the targets of antimalarial drugs, although indirect or off-target physiologic processes, such as transport, sometimes limit our understanding of drug MoA. To identify the target pathways of the Malaria Box compounds, we sought to capture the short-term whole-cell metabolic response of the malaria parasite to these drugs by the use of targeted hydrophilic metabolomics.

Since the advent of global mass spectrometry methods, metabolomics has proven to be a valuable tool in drug development (46–49). Recently, metabolomics has provided a greater understanding of *Plasmodium* parasite metabolite levels and metabolic responses to several common antimalarial drugs (50–55). When paired with quantitative trait locus (QTL) analysis, metabolo-

Received 10 June 2016 **Returned for modification** 25 July 2016
Accepted 16 August 2016
Accepted manuscript posted online 29 August 2016
Citation Allman EL, Painter HJ, Samra J, Carrasquilla M, Llinás M. 2016. Metabolomic profiling of the Malaria Box reveals antimalarial target pathways. Antimicrob Agents Chemother 60:6635–6649. doi:10.1128/AAC.01224-16.

Address correspondence to Manuel Llinás, manuel@psu.edu.

* Present address: Manuela Carrasquilla, Wellcome Trust Sanger Institute, Wellcome Genome Campus, Hinxton, Cambridgeshire, United Kingdom.

E. L. Allman and H. J. Painter share first authorship and contributed equally to this article.

Supplemental material for this article may be found at http://dx.doi.org/10.1128/AAC.01224-16.

For a companion article on this topic, see doi:10.1128/AAC.01226-16.

TABLE 1 Validation compounds and chemical and target information for the selected validation compounds

Compound ID[a]	Putative target/mode of action[b]	Compound class	Reference
ELQ-300*	bc_1 complex	4(1*H*)-Quinolone	84
Antimycin A	bc_1 complex (Q_i site)	Other	119
Atovaquone	bc_1 complex (Q_o site)	Naphthoquinone	61
Myxothiazol	bc_1 complex (Q_o site)	Other	120
P218*	DHFR	2,4-Diaminopyrimidine	89
Pyrimethamine	DHFR	Antifolate	87
WR99210	DHFR	Antifolate	88
DSM265*	DHODH	Triazolopyrimidine	86
DSM1	DHODH	Triazolopyrimidine	121
2-Deoxyglucose	Hexokinase and phosphoglucoisomerase	Other	122
OZ277*	Peroxide mediated	Trioxane	123
OZ439*	Peroxide mediated	Trioxane	95
KAE609*	*Pf*ATP4	Sprioindolone	36
(+)-SJ733*	*Pf*ATP4	Dihydroisoquinolone	64
KAF246	*Pf*ATP4	Spiroindolone	37
KAF156*	*Pf*CARL	Imidazolopiperazine	39
Chloroquine	*Pf*CRT	4-Aminoquinonlone	124
MMV390048*	*Pf*PI4K	Aminopyridine	91
DDD498*	Translation elongation factor 2	Quinoline-4-carboxamide	40
AZ412*	Vacuolar ATP synthase (V-type H+-ATPase) subunit D	Triaminopyrimidine	92

[a] MMV lead compounds are denoted with an asterisk.
[b] DHFR, dihydrofolate reductase; DHODH, dihydroorotate dehydrogenase.

mic profiling has revealed that peptide accumulation mediates fitness costs associated with chloroquine resistance (51). Additionally, metabolomics has aided in the elucidation of novel elements of *Plasmodium* biology, such as the production of plant-like terpenes through the isoprenoid biosynthesis pathway (56), the availability of a diverse pool of host metabolites in reticulocytes compared to mature erythrocytes (57), and rapid arginine depletion *in vitro*, which may be the basis for clinical hypoargininemia (54). More recently, a number of studies have utilized untargeted metabolomics analysis to characterize the mode of action of drugs in other related parasites (58, 59). Despite advances in parasite-based approaches, metabolomics has not been adopted for large-scale antimalarial screening efforts and prior studies have not capitalized on the full potential of the analytical platform focusing only on a few pathways, a limited number of drugs, or specific parasite stages (50–52, 54, 55, 60).

In the present study, we used a medium-throughput targeted ultra-high-performance liquid chromatography–mass spectrometry (UHPLC-MS)-based hydrophilic metabolomics method to determine the specific metabolic signatures arising following treatment of *P. falciparum* asexual blood stage trophozoites with select pharmaceuticals. To assess the metabolic effects of antimalarial treatment and optimize our methodology, we used the known bc_1 complex inhibitor atovaquone (61). We then applied this metabolomic profiling method to 9 well-characterized drugs and 11 lead antimalarial compounds with known or proposed targets from the MMV pipeline (Table 1), as well as the drug-like compounds from the Malaria Box. Based on hierarchical clustering of the resulting metabolomic profiles and the identification of perturbations in a specific metabolic pathway(s), compounds were largely classified into four major categories: mitochondrial electron transport (mtETC)/pyrimidine biosynthesis, folate biosynthesis, hemoglobin catabolism, and cellular homeostasis. The cellular homeostasis category is of particular interest as it encompasses all of the MMV lead and Malaria Box drug-like compounds recently demonstrated to affect *Pf*ATP4, a plasma membrane P-type Na^+/H^+-ATPase (38, 62–64). In addition to these distinct categories, there were a number of Malaria Box compounds that could not be classified because they resulted in a broad or ambiguous metabolomic profile under the conditions tested. As a proof of concept, we also show that our whole-cell method can be utilized to characterize metabolic changes in the sexual-stage gametocyte following drug exposure. Even though transmission blocking is widely considered an essential target for the elimination of malaria, few frontline antimalarial drugs successfully target gametocytes (65), emphasizing the need to extend the application of our assay toward defining gametocytocidal modes of action. Ultimately, this study supports the predicted target pathway(s) for most lead MMV pipeline compounds and provides the malaria community with potential MoAs for a majority of Malaria Box drug-like compounds, highlighting the potential of metabolomic profiling methods for the development of future antimalarial therapeutics.

MATERIALS AND METHODS

Parasite culture maintenance. *Plasmodium falciparum* strain 3D7 (Malaria Research and Reference Reagent Resource Center [MR4, https://www.beiresources.org/MR4Home.aspx]; catalog no. MRA-102) was maintained under standard conditions (66) at 2% hematocrit with O-positive human erythrocytes in RPMI 1640 (Thermo Fisher Scientific) containing 10 mg/liter hypoxanthine, 2 g/liter sodium bicarbonate (Sigma-Aldrich), 15 mM HEPES (Sigma-Aldrich), 50 mg/liter gentamicin sulfate (Sigma-Aldrich), and 2.5 g/liter AlbuMAX II (Thermo Fisher Scientific). Intraerythrocytic ring-stage developing parasites were suspended in 5% sorbitol (Sigma-Aldrich) over three subsequent developmental cycles to synchronize parasites within 4 to 6 h, as previously described (67). Briefly, *P. falciparum* cultures were collected by centrifugation at 1,500 × *g* for 5 min at 25°C, and the parasitized red blood cell (RBC) pellet was resuspended in a 10× volume of 5% sorbitol, followed by incubation at 37°C for 10 min. Following incubation, the cells were pelleted as described

above and washed in 50 ml of complete medium, prior to placement of the parasites back into culture flasks at 2% hematocrit and 2% parasitemia.

Parasite cultures were maintained mycoplasma-free and were confirmed (by PCR) prior to metabolomics analysis. Separate mycoplasma-free culture apparatus and solutions were used for all metabolomics culturing to prevent contamination. Cultures were checked for mycoplasma contamination weekly using an IntronBio *e*-Myco mycoplasma PCR detection kit (Boca Scientific catalog no. 25235).

Method optimization using atovaquone. (i) Stage. At 10 (ring), 24 (trophozoite), and 38 (schizont) h postinvasion (hpi), parasites (10% parasitemia, 5% hematocrit) were treated with atovaquone (kindly provided by Akhil B. Vaidya, Drexel University College of Medicine, Philadelphia, PA) at 10× IC_{50} (where IC_{50} is 50% of the maximum growth inhibitory concentration) (10 nM) for 2.5 h in parallel with an untreated parasite culture and an uninfected erythrocyte control. Posttreatment, 1.5 ml of parasites was lysed with saponin (Acros Organics; 0.02%) for 30 s, collected by centrifugation at 5,000 rpm at 25°C, and resuspended in ice-cold 1× phosphate-buffered saline (PBS) for metabolite extraction.

(ii) Parasite preparation. At 24 hpi, parasites (10% parasitemia, 5% hematocrit) were treated with atovaquone at 10× IC_{50} (10 nM) for 2.5 h in parallel with an untreated parasite culture, an uninfected erythrocyte control, and magnetically purified parasites (both treated and untreated). Following treatment, 1.5 ml each of culture suspensions of treated and untreated parasites was centrifuged in an Eppendorf tube for 30 s at 5,000 rpm at 25°C. The supernatant was removed, and the parasitized RBC pellet was then resuspended in 1.0 ml of 1× PBS. For measurement of metabolites in "bulk culture" (parasitized and nonparasitized RBCs), these parasite suspensions were then placed on ice for metabolite extraction. Alternatively, to remove background erythrocyte metabolite contamination, the parasites were lysed with 0.02% saponin for 30 s, followed by centrifugation for 30 s at 5,000 rpm at 25°C and supernatant aspiration. Isolated parasite pellets were then resuspended in 1.0 ml of ice-cold 1× PBS for metabolite extraction. Magnetic purification was performed as described below, and extraction was performed following centrifugation and supernatant removal as described above. The various extraction methods were performed in triplicate for two biological replicates.

(iii) Concentration. At 24 hpi, parasites were synchronized and magnetically purified as described below. After a 1- to 2-h period of recovery, parasites (~1.5×10^8 per treatment condition) were then treated with atovaquone at 1× (1.0 nM), 2× (2.0 nM), 5× (5.0 nM), 10× (10 nM), 20× (20 nM), and 50× IC_{50} (50 nM) for 2.5 h or no drug was added. All treatments were carried out in triplicate and performed for two biological replicates.

(iv) Time. At 24 hpi, parasites were synchronized and magnetically purified as described below. After a 1- to 2-h period of recovery, parasites (~1.5×10^8 per treatment condition) then were either left untreated or treated with atovaquone at 10× IC_{50} (10 nM) for 0.5, 1.0, 2.0, 4.0, and 8.0 h. Data at all time points were collected in triplicate, and treatments were performed for two biological replicates.

Magnetic column separation. Magnetic separation of mature trophozoites (24 to 36 hpi) was carried out as previously described (68, 69) using an in-house-constructed magnetic cell fractionation system. Upon purification, parasites were allowed to recover under standard culture conditions at 0.5% hematocrit for 1 to 2 h before experimentation.

Sample preparation for antimalarial metabolite profiling. Drug treatments were typically performed on six compounds per trial, with an atovaquone treatment as a positive control and a paired untreated control. Briefly, magnetically purified parasites (20- to 30-μl pellet) were incubated in 6-well plates at 0.5% hematocrit with antimalarial compounds at >2× IC_{50} for 2.5 h. The concentration used was subject to compound availability, and not all Malaria Box drug-like compounds could be tested due to limited quantities. Immediately following each treatment trial, infected erythrocytes were quickly pelleted by centrifugation for 30 s at 5,000 rpm at 25°C, medium was removed, and cells were extracted as described below.

Metabolite extraction. Extractions were performed as described previously (50, 60). Briefly, an ~20-μl pellet of cells was resuspended in 1.0 ml of prechilled 90:10 methanol-water and placed at 4°C. The internal standard [$^{13}C_4$,$^{15}N_1$]aspartate was spiked into the extraction methanol solution to control for sample preparation and handling. Samples were vortexed, resuspended, and centrifuged for 10 min at 15,000 rpm and 4°C. To minimize variation and stabilize metabolites, supernatants were collected and stored at −80°C for less than 1 month or dried down immediately under nitrogen flow for UHPLC-MS analysis. The dried metabolites were resuspended in HPLC-grade water (Chromasolv; Sigma) to a concentration between 1.0×10^5 and 1.0×10^6 cells/μl, based on hemocytometer counts of purified parasites. All samples were processed in triplicate with method blanks to reduce technical variation and account for background signal. Samples were randomized, and 10 μl of resuspended metabolite extract or method blank was injected for UHPLC-MS analysis.

Gametocyte culturing. Culturing of *P. falciparum* 3D7 for gametocyte production was performed using established methods (50). Gametocyte induction of an asexual ring stage culture was performed through volume expansion (2×) without the removal of the "spent" medium, resulting in a hematocrit reduction and a 50/50 spent/fresh medium mix (day −1). On day +1, the medium was replaced in cultures now containing a mixture of asexual and sexual ring stages. On day +2, cultures were given fresh medium containing 50 mM *N*-acetylglucosamine (NAG) to block subsequent asexual replication and to enrich for nonreplicating gametocytes. Giemsa-stained thin blood smears were prepared and examined on day +3 to ensure the absence of asexual ring stage parasites, and the medium was changed daily in the absence of NAG. On day +6, the culture contained mostly stage III-IV gametocytes, which were magnetically purified and processed by following the protocol described above. These gametocytes were treated with 1.0 μM atovaquone for 2.5 h, followed by metabolite extraction as described above.

UHPLC-MS measurement of whole-cell metabolic extracts. Extracts were analyzed using reversed-phase ultra-high-performance liquid chromatography–mass spectrometry (UHPLC-MS) on a Thermo Exactive Plus orbitrap. Metabolite separation was performed with a C_{18} column (Phenomenex Hydro-RP; catalog no. 00D-4387-B0) using a 25-min gradient of 3% aqueous methanol–15 mM acetic acid–10 mM tributylamine ion pairing agent (A) and 100% methanol (MeOH) (B) (70). Detection was performed in negative-ion mode, using a scan range of 85 to 1,000 *m/z* and a resolution of 140,000 at *m/z* 200. Calibration was performed prior to every acquisition batch, using Pierce negative ESI calibration solution (Thermo Fisher Scientific), and glucose-free RPMI 1640 without Albumax II was routinely run as a quality assurance sample to monitor analytical performance. Additional sample randomization was also performed to reduce within-batch variability. To aid in the detection of cellular metabolites, a database was generated from 242 pure metabolite standards using the same instrument and method to determine detection capability, mass/charge ratio (*m/z*), and retention time for each metabolite (see Table S1 and Fig. S1 in the supplemental material for metabolome coverage) (71, 72).

Data analysis. Raw data files from the Thermo Exactive Plus orbitrap (.raw) were converted to a format compatible with our analysis software (.raw →.mzXML) (68, 73). Spectral data (.mzXML files) were visualized in MAVEN (74), the heavy-labeled [$^{13}C_4$, $^{15}N_1$]aspartate internal standard intensity was assessed for technical reproducibility, and peaks for each metabolite in the targeted library were identified based on proximity to standard retention time, the observed mass falling within 10 ppm of the expected *m/z* (calculated from the monoisotopic mass), and the signal/blank ratio (minimum, 10,000 ions). Based upon the above criteria, peaks were manually inspected and demarcated as good or bad based on peak shape. Peak areas were exported into an R working environment (http://www.R-project.org) (75) for calculation of $\log_2$ fold changes for each sample compared to an untreated control. Metabolites that were not reliably detected across 90% of all the trials were removed prior to additional analysis to minimize subsequent imputation bias (76). The peak areas for

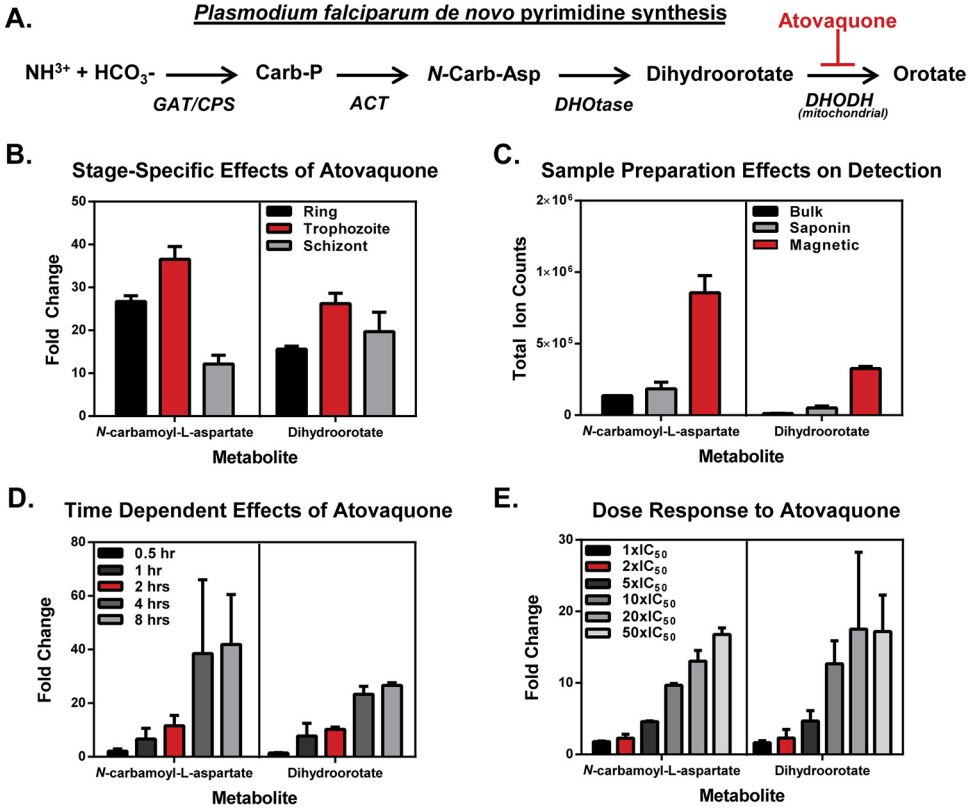

FIG 1 Optimization of whole-cell metabolomic profiling using the bc_1 complex inhibitor atovaquone. (A) The *P. falciparum de novo* pyrimidine biosynthesis pathway. Inhibition of the bc_1 complex by atovaquone is shown in red and denotes the blockage in conversion of dihydroorotate to orotate following mitochondrial electron transport disruption. (B) Parasites were treated with atovaquone (10× IC_{50}) at the ring, trophozoite, and schizont stages of intraerythrocytic development. The resulting fold change in ion counts for *N*-carbamoyl-L-aspartate and dihydroorotate relative to an untreated control is shown. (C) Trophozoite stage cultures were treated with atovaquone (10× IC_{50}) and extracted either in bulk (infected RBCs and uninfected RBCs), as saponin-lysed parasites, or as magnetically purified parasites. The absolute signal was determined using the average total ion counts for *N*-carbamoyl-L-aspartate and dihydroorotate. (D) Magnetically purified trophozoites were treated with atovaquone at 10× IC_{50} for 0.5, 1, 2, 4, and 8 h. The parasite response over time was assessed by measuring the fold change accumulation of *N*-carbamoyl-L-aspartate and dihydroorotate relative to an untreated control. (E) Magnetically purified trophozoites were treated with atovaquone at 1×, 2×, 5×, 10×, 20×, and 50× IC_{50} atovaquone for 2.5 h. The concentration-dependent inhibition was monitored using the *N*-carbamoyl-L-aspartate and dihydroorotate response relative to an untreated control. For each atovaquone concentration, three independent biological replicates were assayed with 3 drug-exposed and 3 untreated samples for each. Values are experimental averages ± standard deviations (SD). The red bar in each graph represents the optimal condition chosen for the experimental workflow (see Fig. 2A). NH^{3+}, ammonia; HCO_3^-, bicarbonate; Carb-P, carbamoyl phosphate; *N*-Carb-Asp, *N*-carbamoyl-L-aspartate; GAT, glutamine amidotransferase; CPS, carbamoyl phosphate synthase; ACT, aspartate carbamoyl transferase; DHOtase, dihydroorotase; DHODH, dihydroorotate dehydrogenase.

any remaining metabolites not detected were imputed to have 10,000 ions, and metabolites detected below background levels (negative after blank subtraction) were maintained as "0" prior to averaging and $\log_2$ calculation. Since our metabolite extraction method did not include a wash step, metabolites found in the RPMI medium were excluded.

The $\log_2$ fold changes of detected metabolites from the validation drugs were used to train a self-organizing map (SOM), and a two-dimensional hexagonal fingerprint was generated for each drug by projection onto the trained map with the supraHex package for R/Bioconductor (77). These suprahexagons display related metabolites within nodes or small hexagons that are arranged radially outward from the center based on vector weight. This organizational pattern places the most influential metabolite nodes on the outer edge of the suprahexagon while preserving the input data information such as the dimensionality, distribution, distance, clusters, and identity of metabolites (see Fig. S2B to E and Table S3 in the supplemental material). The validation data set was used to generate the base metabolic fingerprint or "metaprint," against which all additional metabolite data from the Malaria Box and gametocytes were projected. A subset of compounds from the validation set that gave a strong signature was used to assist in the classification of parasite metabolic perturbation to MMV Malaria Box compounds. Hierarchical clustering was performed on the $\log_2$ fold change values using Pearson-Ward clustering. All processed metabolomics spectral data and analytical metadata from this study have been deposited into the NIH Metabolomics Workbench (project ID no. PR000340).

RESULTS

Experimental optimization for metabolomic profiling. In this study, our goal was to capture and compare the metabolomic profiles of blood stage *P. falciparum* parasites following treatment with a broad range of antimalarial drugs. Therefore, we first optimized a number of methodological parameters using the established antimalarial drug atovaquone. Atovaquone is a direct inhibitor of the *Plasmodium* bc_1 complex (61), an essential component of the mitochondrial electron transport chain (mtETC). Inhibition of the bc_1 complex results in the disruption of ubiquinone recycling, ultimately reducing levels of this cofactor below what is necessary for *de novo* pyrimidine synthesis (Fig. 1A) (50, 61, 78, 79). When parasites were treated with atovaquone, a

rapid, robust, and highly reproducible increase was detected in the pyrimidine biosynthesis precursors *N*-carbamoyl-L-aspartate (*N*-Carb-Asp) and dihydroorotate (DHO), in comparison to that of an untreated control (Fig. 1B), reflecting indirect inhibition of dihydroorotate dehydrogenase (Fig. 1A). Therefore, we used this signature of metabolic disruption in *de novo* pyrimidine synthesis to optimize several parameters for testing subsequent compounds. First, we measured metabolic changes in total parasite cultures at different stages of intraerythrocytic development by exposing highly synchronous *P. falciparum* 3D7 parasites to atovaquone (10× IC_{50}) at the ring, trophozoite, and schizont stages of asexual growth. Our UHPLC-MS data demonstrated that the highest fold change in *N*-Carb-Asp and DHO (Fig. 1B) occurred during the trophozoite stage of development. In addition to confirming that disruption of pyrimidine biosynthesis is the biochemical consequence of atovaquone treatment (50, 78), this result demonstrates that the highly metabolically active trophozoite results in the best overall signal intensity and supports the use of whole-cell metabolomics at this stage of development.

Having defined the appropriate stage of parasite development to focus on, we next identified the sample preparation resulting in the most robust and reproducible metabolic signature upon atovaquone exposure. By comparing the responses in *N*-Carb-Asp and DHO from the same number of parasites from an atovaquone-treated pelleted bulk culture, saponin-lysed parasites, or magnetically purified trophozoite-infected erythrocytes, we found that magnetic purification led to the largest absolute signal intensity in *N*-Carb-Asp and DHO (Fig. 1C). We then determined the optimal range for drug incubation time by comparing magnetically purified atovaquone-treated and untreated parasite metabolite extracts after incubations of 0.5, 1, 2, 4, and 8 h and observed a time-dependent accumulation of *N*-Carb-Asp and DHO (Fig. 1D). In order to capture the most immediate, yet robust metabolic response, 2.5 h of treatment was selected as an intermediate value within the optimal range, particularly since longer treatments led to increased variability that was possibly due to parasite developmental transition to schizogony (Fig. 1D). Notably, our assay demonstrated the rapid and robust capture of metabolic disruption after treatment, even though atovaquone is known to have a low parasite-killing rate (>24 h) (80–82). These findings support previous observations that bc_1 inhibitors result in rapid inhibition of oxygen consumption and *de novo* pyrimidine metabolism, which are direct precursors of parasite death (78, 79, 83, 84).

Lastly, we determined the minimum concentration of drug required to observe the characteristic metabolic signature of atovaquone treatment within this 2.5-h incubation time. Magnetically purified parasites were treated with atovaquone at 1×, 2×, 5×, 10×, 20×, and 50× IC_{50} (Fig. 1E), and all concentrations at or above the IC_{50} resulted in the buildup of the signature metabolites, *N*-Carb-Asp and DHO. In short, atovaquone allowed us to determine the concentration range of drug to be used, the time of exposure, the parasite life stage, and the optimal purification method which defined the workflow for assaying the parasite-specific response to a broad range of characterized and uncharacterized drugs (Fig. 2A). This was a pragmatic and reasonable decision given that the mode of action of a new compound may impact these parameters and that optimization of conditions for each individual case was not feasible.

Validation of experimental workflow using well-characterized drugs. Using the optimized experimental conditions described above, we first tested our method on nine well-established drugs and 11 "next-generation" MMV lead antimalarials (Table 1). This group of compounds was chosen as a validation set to demonstrate that UHPLC-MS metabolomics is capable of detecting the biochemical pathway affected by antimalarial drugs beyond those that disrupt mitochondrial function and pyrimidine synthesis. These 11 compounds have been studied extensively using a variety of approaches, and tentative targets have been previously identified (Table 1). In order to remove any potential for bias from this prior knowledge, our initial treatment and data analysis of the validation compounds were carried out in a blind fashion by arbitrarily numbering the compounds prior to metabolomics analysis. This test was critical to establish the predictive power of our methodology by allowing us to deduce the target pathway(s) for these compounds through the metabolomic profiles alone. To identify the metabolic changes occurring in response to drug treatment, we performed targeted peak picking from a database of known metabolites. This database contained the retention times and chemical formulas for 242 standards analyzed on the same analytical platform (see Table S1 in the supplemental material). These standards span a large portion of the known parasite metabolome with a focus on hydrophilic cellular metabolites (see Fig. S1 and Table S1) (71, 72). By UHPLC-MS, we reliably and consistently detected 113 targeted hydrophilic metabolites in greater than 90% of parasite extracts, and the $\log_2$ fold changes in the peak areas, compared to an untreated control, were used to elucidate the effect of each individual particular drug (see Fig. S2A and Table S2).

To visualize specific metabolic perturbations associated with each drug, the $\log_2$ fold change values (see Table S2 in the supplemental material) were assembled using a self-organizing map (SOM) and projected onto a suprahexagonal landscape (Fig. 2B; see Fig. S2B to E and Table S3) (77). The resulting map displays the "metabolic fingerprint" or metaprint for a particular treatment and provided us with a straightforward way of displaying cellular metabolic changes for any given drug and to easily compare phenotypes between compounds (Fig. 2B). The metaprints resulting from treatment with an individual compound may have patterns of metabolic perturbation that resemble the responses from other drugs but are never exactly the same, just as no two fingerprints are identical. Compounds that display a similar metaprint pattern cluster well together and therefore likely target similar biochemical pathways (Fig. 2C). Examination of the metabolite identities within the metaprint (see Fig. S2B and Table S3) revealed four clear metabolic "signatures" that are distinguished by perturbations in folate biosynthesis, cellular homeostasis, mtETC/pyrimidine synthesis, or hemoglobin catabolism (Fig. 2C). Additionally, an unclassified cluster which displayed either a broad or ambiguous profile and consequently lacked "signature" metabolites was present. When the drug identities were ultimately disclosed, we found that compounds with the same predicted target clustered together, as expected. For example, atovaquone (control), antimycin A, myxothiazol, and ELQ-300, which all inhibit the bc_1 complex, share a cluster, as do KAE609, (+)-SJ733, and KAF246, which are known to alter *Pf*ATP4 function (Fig. 2C and Table 1). Specifically, metabolites with the highest variance (mapping to the edges) (see Fig. S2F) reveal metabolic signatures within the validation set and relate accordingly to the expected molecular target of each drug (Fig. 2C and Table 1).

The *Plasmodium* metaprints resulting from drug treatment

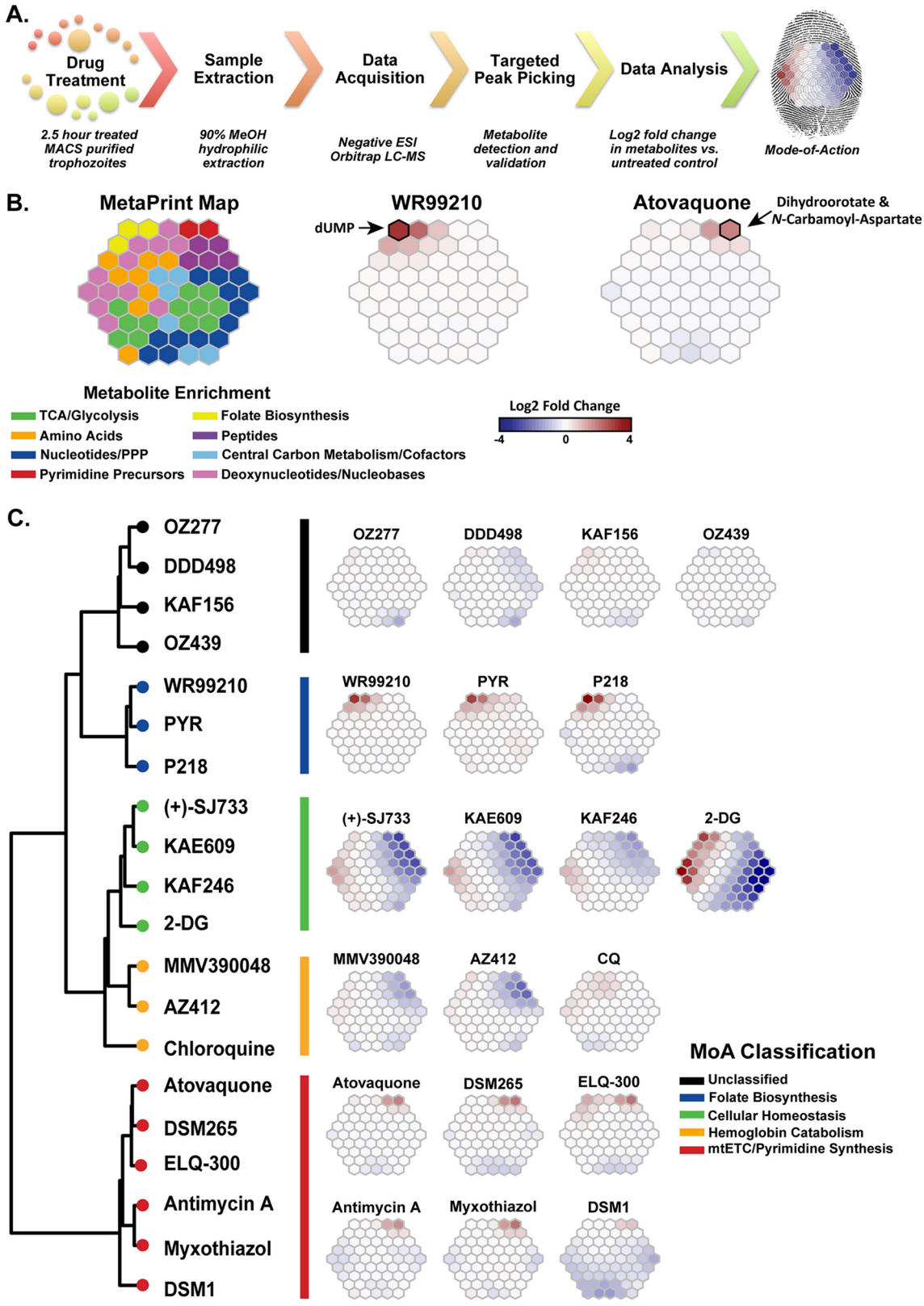

FIG 2 Metabolomic fingerprint analysis of validated compounds with antimalarial activity. (A) Experimental metabolomic profiling pipeline used for all validation and MMV Malaria Box experiments, based on parameters determined from results shown in Fig. 1. (B) Metabolomic profiling was used to measure the parasite metabolic response following drug treatment (see Table S2 in the supplemental material). The data were analyzed using self-organizing maps and are displayed as a suprahexagonal (66) metabolic fingerprint or metaprint. Metabolite clusters were associated with eight generalized metabolic pathways using the KEGG database and were color coded within the suprahexagon base map (left). Metaprints for both atovaquone and WR99210 are displayed as examples, with specific signature metabolites denoted (right). (Mapping locations for all metabolites can be found in Table S3.) (C) We assembled metaprints (right) and clusters (Pearson-Ward distance-clustering) (left) based on the metabolomic profiles for each compound, as determined from the $\log_2$ fold change values of targeted metabolites following drug treatment relative to an untreated (no-drug) control (see Table S2). MoA classifications were performed based on a combination of clustering, metaprint analysis (right), and *a priori* biochemical knowledge (Table 1). Pyr, pyrimethamine; 2-DG, 2-deoxyglucose; CQ, chloroquine.

demonstrate that all known bc_1 complex inhibitors (Table 1) have metabolic effects that result in large increases of DHO and *N*-Carb-Asp, as well as smaller decreases in downstream pyrimidine nucleotides (Fig. 2C; see Table S2 in the supplemental material). A similar metabolic response was seen for DSM1 (85) and DSM265 (86), which directly inhibit mitochondrial dihydroorotate dehydrogenase (DHODH) (Fig. 2C and Table 1), highlighting the essential linkage between mtETC and pyrimidine synthesis. However, treatment with ELQ-300 and DSM265 resulted in a higher fold increase in pyrimidine precursors with a coordinated decrease in nucleotides (Fig. 2B), suggesting a more robust perturbation to parasite *de novo* pyrimidine synthesis than is generated by atovaquone likely due to the high selectivity of these compounds (84, 86). Although targeted metabolomics analysis revealed perturbations of pyrimidine synthesis, we were unable to distinguish whether the changes arose from indirect inhibition at the bc_1 complex Q_o or Q_i semiquinone electron transfer sites or direct DHODH blockage (Table 1; Fig. 2B, red cluster) and are listed as general inhibitors of mtETC/pyrimidine synthesis.

Also clustering together are P218, pyrimethamine, and WR99210 (Fig. 2C), all of which target the bifunctional *Plasmodium* enzyme dihydrofolate reductase-thymidylate synthase (DHFR-TS), which is responsible for the folate-dependent conversion of dUMP to dTMP (87–89). Treatment with these compounds results in an increase in dUMP and NADPH (Fig. 2C; see Table S2 in the supplemental material), clearly demonstrating inhibition of DHFR-TS, which also utilizes NADPH as a cofactor. This distinct metabolic signature represents disruption of folate biosynthesis and supports the known target pathway of the lead MMV compound P218 (89), further confirming DHFR-TS as a prime antimalarial drug target.

Compounds KAE609, (+)-SJ733, and KAF246 have been suggested to target *Pf*ATP4 (36, 38, 64), an Na^+/H^+-ATPase in the parasite plasma membrane (63). However, the exact mechanism causing parasite death from these compounds remains unknown. Recently, treatment with the *Pf*ATP4 inhibitor KAE609 was demonstrated to result in a rapid influx of Na^+, inducing plasma membrane rigidification, which potentially results in premature developmental progression and, ultimately, parasite death (90). Metaprints reveal a widespread metabolic disruption likely resulting from the physiologic loss of the ionic gradient generated by *Pf*ATP4 and perturbations to parasite development. Treatment with these compounds results in multiple, likely indirect, metabolic effects, as evidenced by increases in deoxyribonucleotides and decreases in central carbon metabolites, ribonucleotides, hemoglobin-derived peptides, and amino acid derivatives (Fig. 2C; see Table S2 in the supplemental material). Within this cluster, metaprints for these *Pf*ATP4-targeting compounds do display differences from that of 2-deoxyglucose (2-DG) (Fig. 2C), a compound known to competitively inhibit glycolysis and ATP production, resulting in a direct yet widespread metabolic collapse distinct from the *Pf*ATP4-derived metaprint. Due to the broad or multiple metabolic signatures revealed by metaprint analysis, the MoA as determined by whole-cell metabolomics for compounds in this class could not be precisely classified without prior knowledge and are thus listed as disruptions to cellular homeostasis.

The next cluster contains the phosphatidylinositol 4-kinase (PI4K) inhibitor MMV390048 (91), the putative vacuolar ATPase-targeting compound AZ412 (92), and chloroquine, which accumulates within the digestive vacuole of chloroquine-sensitive *Plasmodium* parasites. All compounds within this cluster reveal a unique signature consisting of perturbations in hemoglobin-derived peptides and amino acid derivatives (Fig. 2C; see Table S2 in the supplemental material). Although these compounds have a broad range of predicted molecular targets, their metabolic signatures suggest that they all perturb parasite hemoglobin catabolism. Previous studies have established that *Plasmodium* survival is dependent upon the catabolism of hemoglobin to peptides/amino acids and their active transport from the digestive vacuole, a process that is mediated by the chloroquine resistance transporter (*Pf*CRT) and inhibited by chloroquine (93). The metaprints of the compounds within this cluster confirm the parasite's reliance on a constant supply of peptides/amino acids from the host erythrocyte for survival and are categorized as inhibitors of hemoglobin catabolism. However, it is important to note that even though chloroquine clusters with this group, the resulting metaprint is quite divergent. This is possibly due to an overall lack of significant metabolic changes, which was previously demonstrated for chloroquine over treatment lengths ranging from 30 min to 24 h (50).

The final cluster includes KAF156, a compound with *Pf*CARL as the resistance marker (39, 41, 94), the known translation inhibitor DDD498 (40), and two aryl trioxolanes, OZ439 and OZ277 (95) (Fig. 2C). Interestingly, the trioxolanes are thought to promote oxidative damage to the parasite (96), similarly to dihydroartemisinin (97), yet display no major alterations in parasite metabolism. While there are small perturbations in NAD metabolism, the changes in redox state within the parasite are difficult to capture using our current metabolomics approach. KAF156 similarly displays little disruption in parasite metabolism, which was not surprising given the limited knowledge about the biological target of this drug (39, 41). Interestingly, the most robust metabolic response in this cluster results from treatment with DDD498, characterized by small perturbations in nucleotides and hemoglobin-derived peptides possibly resulting from the disruption of parasite translation (40, 41). However, due to the overall lack or weakness of a signature in this cluster of compounds, they are tentatively listed as unclassified for this analysis.

Metabolic profiling of Malaria Box drug-like compounds. Reassured by the predictive power of our metabolomic profiling assay from our blind analysis of the validation set of compounds, we applied our approach to a large subset of the drug-like compounds from the Malaria Box (4). Due to the medium-throughput nature of our metabolomics workflow and the limited availability of compounds within the Malaria Box, the treatment and metabolite extraction protocol was performed on 169 of the 200 drug-like compounds over the course of 26 independent drug treatment assays. To ensure consistency, all drug screens were performed according to our optimization scheme (Fig. 1) by treating magnetically purified parasites for 2.5 h at $\geq 2\times$ IC_{50} and were paired with an untreated negative control, as well as an atovaquone-treated positive control for additional experimental quality assurance (Fig. 1 and 2A). All samples within a trial were performed in triplicate to reduce within-run technical variation, and both a single isotope-labeled internal standard ([$^{13}C_4$,$^{15}N_1$]aspartate) and the atovaquone metabolite signature were monitored to determine whether an experimental batch was of acceptable quality for further analysis. Ultimately, this resulted in 31 biological replicates of atovaquone, which aided in the confirmation of the most reliably detected metabolites. The signature metabolites for atovaquone-positive con-

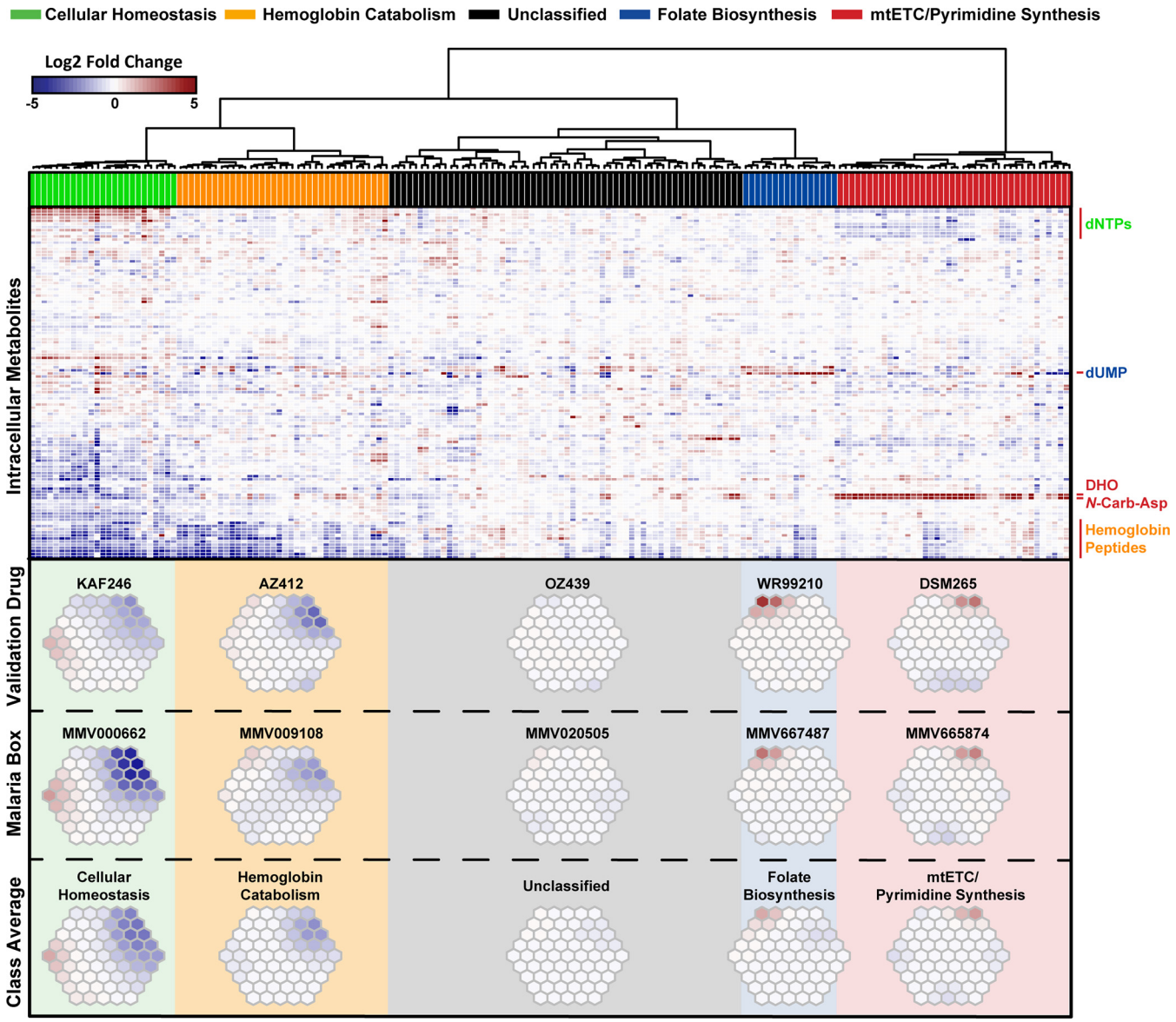

FIG 3 Metabolomic profiling of Malaria Box drug-like compounds. Heat map of $\log_2$ fold change values of 113 metabolites, relative to a no-drug control, for 169 drug-like compounds from the Malaria Box and several selected validation compounds from each MoA classification (top). All the displayed $\log_2$ fold changes are the averages for three technical replicates for each compound tested. Distance clustering was performed using the Pearson-Ward method. Selected metabolites are denoted on the right, corresponding to specific metabolic signatures within a particular MoA class, and are color coded. Metaprints (bottom) are included for visualization of the metabolomic profiles associated with each MoA class and contain a validation compound (see Fig. 2C, e.g., KAF246), an MMV Malaria Box representative (e.g., MMV000662), and an average representation of all metabolites within each MoA classification cluster. Metaprint data for the MMV Malaria Box compounds match the map legend in Fig. 2A and Table S3 in the supplemental material since all data were overlaid onto the trained validation set map. The full data set and metaprints are available in Tables S3 and S4, respectively. DHO, dihydroorotate; *N*-Carb-Asp, *N*-carbamoyl-L-aspartate.

trols, *N*-Carb-Asp and DHO (Fig. 1 and 2), across all drug tests provided robust and reproducible fold changes that were >4-fold in all experiments (data not shown).

Surprisingly, hierarchical clustering analysis of the $\log_2$ fold change compared to an untreated control for the entire set of 169 Malaria Box compounds also revealed that these drugs largely fell into the same five broad categories based upon their individual metaprints (Fig. 3; see Tables S4 and S5 in the supplemental material). Thirty-eight Malaria Box compounds were categorized as inhibitors of mtETC/pyrimidine biosynthesis (Fig. 3, red) and displayed a prominent increase in *N*-Carb-Asp and DHO, similar to that of atovaquone (Fig. 2B and C; see Tables S4 and S5). Treatment with 23 of the Malaria Box compounds resulted in numerous metabolic changes indicative of perturbations in cellular homeostasis (Fig. 3, green), analogous to those caused by the *Pf*ATP4 inhibitors KAE609, (+)-SJ733, and KAF246 (Fig. 2C). Interestingly, this set of 23 compounds includes all of the Malaria Box drug-like compounds previously identified as targeting *Pf*ATP4 (63), plus an additional six compounds, demonstrating unequivocally that *Pf*ATP4 inhibition and the loss of Na^+/H^+ homeostasis result in a related and distinct metabolic profile. Fourteen Malaria Box compounds clustered in the folate biosynthesis category

(Fig. 3, blue) and displayed a dUMP perturbation similar to that of WR99210, P218, and pyrimethamine (Fig. 2C). Of note, MMV667487 was found in this cluster displaying a marked increase in dUMP. This result confirms a recent chemogenomic screen for decreased sensitivity to Malaria Box compounds using a parasite line in which expression of DHFR-TS was downregulated using a *glmS* ribozyme fusion (98). Thirty-five Malaria Box compounds were classified by a strong peptide signature that is indicative of disruption in hemoglobin catabolism (Fig. 3, orange). As expected, several of the compounds shown to inhibit either beta-hematin formation (17) or metalloaminopeptidase function (11) also fell into this category (Fig. 3; see Table S5), confirming their effects on hemoglobin catabolism. Finally, 59 Malaria Box drugs displayed weak or ambiguous metabolic changes and were listed as unclassified (Fig. 3, black). Interestingly, despite clustering with compounds that affect hemoglobin catabolism in the validation set (Fig. 2C), in the context of the larger Malaria Box data set (Fig. 3), chloroquine clusters with "unclassified" compounds due to its relatively weak metabolic signature. This confirms a previous metabolomics characterization of chloroquine-treated parasites that showed minimal metabolic perturbation (50). Interestingly, compounds that target nonmetabolic processes and/or have been proposed to alter redox status, such as the aryl trioxolanes (OZ277 and OZ439), also cluster in this group and display few distinct metabolic perturbations.

Application to gametocytes. The continued emergence of drug-resistant malaria parasites has not only intensified the need for new antimalarial drugs targeting asexual-stage parasites but also renewed the focus on transmission-blocking strategies (99, 100). Inhibiting the transfer of viable sexual-stage gametocytes from infected human blood to the mosquito vector would both reduce the at-risk population and slow the spread of drug-resistant parasites, critical steps toward malaria eradication. Despite the therapeutic targeting potential of this intraerythrocytic stage, few gametocytocidal compounds are available and the killing assays used to determine gametocytocidal activity have yielded various results (12, 14–16, 32, 34).

To demonstrate that our methodology has the capability to overcome these shortcomings, we tested our metabolomics platform on sexual-stage gametocytes. Using established induction and purification methods (101, 102), we generated sufficient gametocyte numbers (~5×10^7 gametocytes/sample) for metabolomic profiling and applied our existing workflow to test the effects of atovaquone on mid- to late-stage gametocytes (III-IV). We focused on this stage of gametocytogenesis because the parasite is still developing, is metabolically active, and can be readily purified. Although gametocytes are known to have increased mitochondrial metabolism (52, 55), atovaquone has limited gametocytocidal efficacy (103–105). Despite this, when given a moderate dose of atovaquone (1.0 μM) (106), purified gametocytes displayed the classic atovaquone metabolic signature characterized by an increase in pyrimidine precursors (Fig. 4). As expected, this response was reduced (~2-fold change versus ~15-fold change in asexual parasites) when the DHO and *N*-Carb-Asp levels were compared to those of atovaquone-treated asexual parasites (Fig. 4 and 1, respectively). Additionally, metaprint analysis reflected alterations in central carbon metabolism that are likely the result of pharmacologic perturbation of the enhanced metabolism shown by the gametocyte mitochondrion (55). Nevertheless, this proof-of-principle result demonstrates that atovaquone's limited gametocytocidal activity is the result of a reduced effect on the bc_1 complex and pyrimidine biosynthesis, compared to that in asexual parasites. While the molecular mechanism behind this reduced effect remains unclear, our results demonstrate that metabolomic profiling is able to measure even small perturbations that arise from pharmacologic intervention and will also prove useful for testing gametocytocidal compounds.

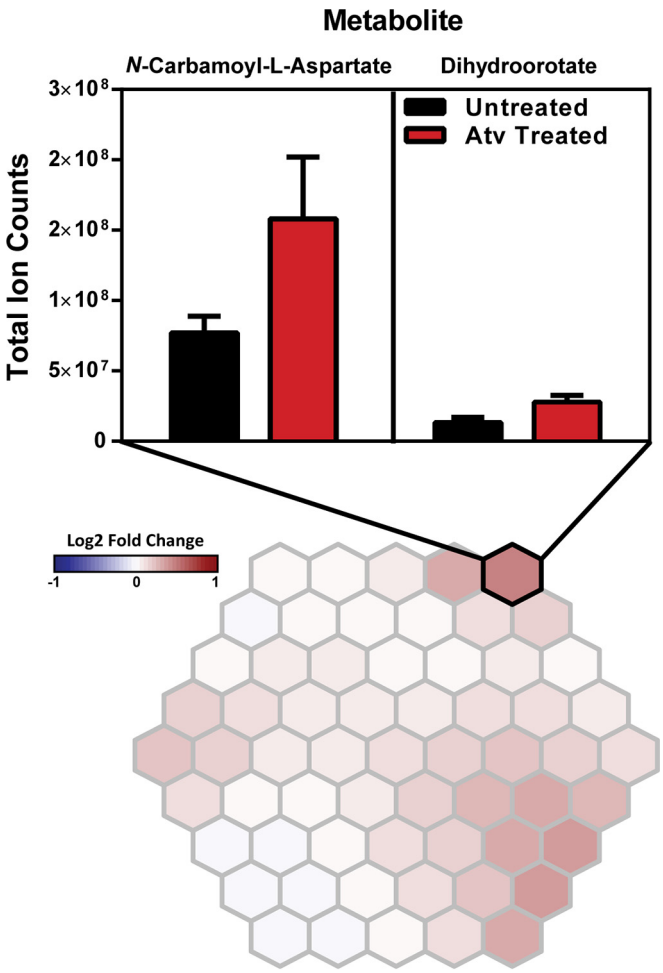

FIG 4 Metabolomic profiling of the *P. falciparum* sexual stage using atovaquone. The metaprint for purified stage III-IV gametocytes treated with 1 μM atovaquone (Atv) for 2.5 h (top) using the same experimental screening approach as that for asexual parasite drug treatment assays (Fig. 2A) is shown. The graph highlights the atovaquone-specific signature, which is much reduced compared to that for asexual-stage parasites (Fig. 1). Two independent biological replicates were assayed with 2 drug-exposed and 2 untreated samples for each. Values displayed are experimental averages ± standard errors. The gametocyte data are available in Table S6 in the supplemental material.

DISCUSSION

This study presents a medium-throughput analysis of 20 well-characterized antimalarial drugs and 169 drug-like candidates from the MMV Malaria Box using targeted metabolomic profiling. Since metabolomics provides a direct chemical signature of the cell, the results provide critical data for many of these compounds that had not been previously identified by endpoint-based approaches. Using optimized treatment parameters (Fig. 1 and 2A), we demonstrated that the target pathways of 20 validated

drugs were correctly classified based on their metabolic fingerprints and that the signature metabolites mapped accurately to the predicted molecular target (Fig. 2 and Table 1). Consequently, this set of drugs provided the necessary framework for predicting the target pathways for ~65% of the screened Malaria Box drug-like compounds (110 of the 169), a number that has not been achieved by other biochemical screens (9–11, 14, 17, 30, 62, 63). Although 35% of the compounds remain unclassified (Fig. 3), our analysis does reveal metabolic perturbations that have yet to be linked to a single metabolic process and will require further investigation.

Targeted trophozoite metabolite profiling of the Malaria Box drug-like compounds revealed the somewhat surprising result that most of the drugs largely fall into four distinct clusters defined by disruptions to mtETC/pyrimidine biosynthesis, folate biosynthesis, hemoglobin catabolism, or global homeostasis, as well as compounds which could not be easily linked to a clear metabolic pathway (Fig. 2 and 3). These results suggest that the parasite may have a limited number of biological functions that are not only necessary for viability but also highly vulnerable to pharmacologic intervention, as previously predicted by modeling the *P. falciparum* metabolic network (107). Each of the four distinct classes were defined by changes to a unique subset of metabolites within the targeted fingerprint known as the "signature." These signatures define the specific pathway(s) disrupted by a particular chemotype. The lack of central carbon disruption in our data, like that seen for 2-deoxyglucose, suggests that these changes in metabolites do not arise from cell death as seen previously in metabolomic perturbation studies in *Plasmodium* (50). Our predicted classifications also agree with several earlier publications in which aminopeptidase/beta-hematin targeting compounds (11, 17) from the Malaria Box displayed a deficiency in hemoglobin-derived peptides (Fig. 3). Additionally, *Pf*ATP4 targeting compounds (62, 64) cluster together and display a clear multifaceted metabolic collapse. However, it is important to note that disruptions to cellular homeostasis from targeting nonmetabolic targets (such as the H^+- and Na^+-ATPases) make exact molecular target prediction from metabolomics difficult without prior biochemical knowledge. We also acknowledge that not all of the compounds show a clear MoA consistent with the published literature. For example, we find that treatment with MMV666693 results in perturbations to mtETC/pyrimidine biosynthesis (Fig. 3), although previous studies have shown that MMV666693 targets translation (10) or kinesin-5 (108). This suggests that there are parameters that need to be carefully considered when making comparisons across experimental approaches, an observation noted previously for endpoint-based assays (12, 33).

One important unknown that remains to be explored is the MoA of the 59 "unclassified" Malaria Box compounds that contain ambiguous or weak fingerprints (Fig. 3). The reasons for these weak metabolomic profiles might include the following: (i) it is possible that we are simply focusing on the wrong subset of metabolites (targeted hydrophilic), (ii) the effects may be more pronounced during another part of the parasite life cycle, (iii) the time of exposure may be too short to exhibit a measurable metabolic effect, (iv) the dose used may be too low (although this is less likely based on our atovaquone data [Fig. 1B to E]), or (v) certain compounds may target broader aspects of parasite biology and therefore display no noticeable metabolic perturbations relative to the control. A related metabolomics approach for determining antibacterial MoAs has also found that compounds that target broad biological processes (i.e., mitochondrial proton transfer) result in limited changes to cellular metabolites (109), in line with our results for DDD498, which targets parasite translation (Fig. 2).

The unclassified group of compounds remains of interest, and expanding our metabolomic methodologies beyond focusing on hydrophilic metabolites may allow us to discern the unique signatures within this class. Interestingly, MMV008138 is among the unclassified compounds, although it is an established inhibitor of the 2-C-methyl-D-erythritol 4-phosphate (MEP) pathway of isoprenoid biosynthesis (14, 30, 110, 111), which is beyond the detection capabilities of our methodology. However, this compound might be used as a known signature of MEP pathway disruption for future analytical optimization. One observation regarding the unclassified compounds was that even though they lacked a defined signature, there were several subclusters forming within these compounds (Fig. 3), suggesting that these drugs may be operating through other MoAs. An untargeted UHPLC-MS approach examining hundreds of additional putative MS features may shed light on some of the compounds not explained by our targeted fingerprinting (112). While untargeted metabolomics is a valuable tool for further defining subcategories of compounds (particularly when combined with the metaprint analysis), it requires rigorous analysis and validation, as well as additional analytical approaches for full metabolic understanding. Furthermore, the use of previous biochemical assays will be important for appropriately guiding additional metabolic experiments and analysis methods as it pertains to this particular compound cluster.

Although asexual screening efforts have been paramount in the effort to identify diverse antimalarial compounds, they only touch on one phase of the parasite's complex life cycle. Recently, added emphasis has been placed on transmission blocking strategies that prevent the transmission of sexual-stage parasites to the mosquito vector. Remarkably, only four antimalarial drugs, methylene blue, artesunate, artemether, and primaquine, kill gametocytes, with primaquine being the only clinically available drug that effectively kills gametocytes (65). Yet the use of primaquine is restricted, as treatment results in hemolysis in glucose-6-phosphate dehydrogenase-deficient individuals (113), a mutation common in many regions where malaria is endemic. To expand our methodology beyond the asexual stages, we tested the metabolic effect of atovaquone on purified mid/late-stage gametocytes (stage III-IV) as a proof of concept. Despite atovaquone's limited efficacy against gametocytes (33, 105), we captured the same pyrimidine biosynthesis signature measured in asexual-stage parasites. While this metabolic signature was markedly reduced (~7-fold), this result emphasizes the power of the platform to capture subtle metabolic perturbations and will aid in determining the MoA of compounds that might be discounted by endpoint assays. To our knowledge, this also marks the first application of metabolomics for the purposes of understanding sexual-stage drug MoA and challenges the historical notion that gametocytes transition to a largely metabolically quiescent state (114–117). However, it has recently been demonstrated that central carbon and mitochondrial metabolism is not only highly active (55) but also essential for gametocytogenesis (52). Therefore, this transmissible stage of development remains a viable and important potential target for chemotherapeutic intervention. To date, several gametocytocidal screens using endpoint-based assays have been performed on the Malaria Box (12–16, 32, 34), identifying a significant number of additional compounds active against this stage. These results further rein-

force that the gametocyte stage is amenable to pharmacologic intervention although the metabolic effects of these compounds on gametocytes remain unknown.

Metabolomic profiling can also be extended into additional aspects of the parasite-drug axis, such as determining the metabolic fingerprints that arise from drug combinations, as this would provide vital information for the real-world development and deployment of frontline combination therapies. Preliminary data from our laboratory suggest that compounds targeting nonoverlapping pathways still manifest their individual signatures, albeit at altered levels (data not shown). Furthermore, a drug-multiplexing approach may allow further identification of compounds that have a synergistic effect, much like that of the atovaquone-proguanil combination. In addition to studying the effects of drugs on parasites, the metabolic network of drug-resistant parasites should be queried to better understand resistance mechanisms and their consequences for the parasite. Having this information will allow optimal combination therapies tailored to prevent the onward transmission of resistance (118), as the parasite would likely be unable to survive disruptions in multiple pathways. In conclusion, our UHPLC-MS metabolomics workflow and antimalarial metabolomic profiling approach provide the parasitology community with data that can be used to help prioritize the next generation of potent antimalarial drugs for future testing in clinical trials.

ACKNOWLEDGMENTS

We thank Andrew D. Patterson and Philip B. Smith of the Penn State Huck Institutes of the Life Sciences Metabolomics Core Facility for analytical expertise, technical oversight, and critical comments, Akhil B. Vaidya, Drexel University College of Medicine, for kindly providing atovaquone, Medicines for Malaria Ventures partners Jeremy Burrows, Didier Leroy, Paul Willis, Thomas Spangenberg, Emilie Burlot, and Benoit Laleu for providing access to compounds, including the MMV Malaria Box, and for helpful discussions, Elizabeth Winzeler, University of California, San Diego, and Brian Yeung, Novartis, for providing KAF246, and Omar Vandal, Bill & Melinda Gates Foundation, for critical discussion and assistance with grant management.

E.L.A., H.J.P., M.C., and J.S. designed and performed experiments and analyzed data. E.L.A., H.J.P., and M.L. wrote the manuscript and generated figures. M.L. designed the experiments and provided critical comments and project oversight.

This project was funded through the generous support of a Bill and Melinda Gates Foundation Grand Challenges Grant (Phase II-OPP1119049).

FUNDING INFORMATION

This work, including the efforts of Manuel Llinás, was funded by Bill and Melinda Gates Foundation (Phase II OPP1119049).

REFERENCES

1. **Miller LH, Ackerman HC, Su XZ, Wellems TE.** 2013. Malaria biology and disease pathogenesis: insights for new treatments. Nat Med **19:**156–167. http://dx.doi.org/10.1038/nm.3073.
2. **RTS,S Clinical Trials Partnership.** 2015. Efficacy and safety of RTS,S/AS01 malaria vaccine with or without a booster dose in infants and children in Africa: final results of a phase 3, individually randomised, controlled trial. Lancet **386:**31–45. http://dx.doi.org/10.1016/S0140-6736(15)60721-8.
3. **Cui L, Lindner S, Miao J.** 2015. Translational regulation during stage transitions in malaria parasites. Ann N Y Acad Sci **1342:**1–9. http://dx.doi.org/10.1111/nyas.12573.
4. **Spangenberg T, Burrows JN, Kowalczyk P, McDonald S, Wells TN, Willis P.** 2013. The open access malaria box: a drug discovery catalyst for neglected diseases. PLoS One **8:**e62906. http://dx.doi.org/10.1371/journal.pone.0062906.
5. **Gamo FJ, Sanz LM, Vidal J, de Cozar C, Alvarez E, Lavandera JL, Vanderwall DE, Green DV, Kumar V, Hasan S, Brown JR, Peishoff CE, Cardon LR, Garcia-Bustos JF.** 2010. Thousands of chemical starting points for antimalarial lead identification. Nature **465:**305–310. http://dx.doi.org/10.1038/nature09107.
6. **Plouffe D, Brinker A, McNamara C, Henson K, Kato N, Kuhen K, Nagle A, Adrian F, Matzen JT, Anderson P, Nam TG, Gray NS, Chatterjee A, Janes J, Yan SF, Trager R, Caldwell JS, Schultz PG, Zhou Y, Winzeler EA.** 2008. In silico activity profiling reveals the mechanism of action of antimalarials discovered in a high-throughput screen. Proc Natl Acad Sci U S A **105:**9059–9064. http://dx.doi.org/10.1073/pnas.0802982105.
7. **Guiguemde WA, Shelat AA, Bouck D, Duffy S, Crowther GJ, Davis PH, Smithson DC, Connelly M, Clark J, Zhu F, Jimenez-Diaz MB, Martinez MS, Wilson EB, Tripathi AK, Gut J, Sharlow ER, Bathurst I, El Mazouni F, Fowble JW, Forquer I, McGinley PL, Castro S, Angulo-Barturen I, Ferrer S, Rosenthal PJ, Derisi JL, Sullivan DJ, Lazo JS, Roos DS, Riscoe MK, Phillips MA, Rathod PK, Van Voorhis WC, Avery VM, Guy RK.** 2010. Chemical genetics of *Plasmodium falciparum*. Nature **465:**311–315. http://dx.doi.org/10.1038/nature09099.
8. **Van Voorhis WC, Adams JH, Adelfio R, Ahyong V, Akabas MH, Alano P, Alday A, Aleman Resto Y, Alsibaee A, Alzualde A, Andrews KT, Avery SV, Avery VM, Ayong L, Baker M, Baker S, Ben Mamoun C, Bhatia S, Bickle Q, Bounaadja L, Bowling T, Bosch J, Boucher LE, Boyom FF, Brea J, Brennan M, Burton A, Caffrey CR, Camarda G, Carrasquilla M, Carter D, Belen Cassera M, Chih-Chien Cheng K, Chindaudomsate W, Chubb A, Colon BL, Colon-Lopez DD, Corbett Y, Crowther GJ, Cowan N, D'Alessandro S, Le Dang N, Delves M, DeRisi JL, Du AY, Duffy S, Abd El-Salam El-Sayed S, Ferdig MT, Fernandez Robledo JA, Fidock DA, et al.** 2016. Open source drug discovery with the Malaria Box compound collection for neglected diseases and beyond. PLoS Pathog **12:**e1005763. http://dx.doi.org/10.1371/journal.ppat.1005763.
9. **Tiwari NK, Reynolds PJ, Calderon AI.** 2016. Preliminary LC-MS based screening for inhibitors of *Plasmodium falciparum* thioredoxin reductase (PfTrxR) among a set of antimalarials from the Malaria Box. Molecules **21:**424. http://dx.doi.org/10.3390/molecules21040424.
10. **Ahyong V, Sheridan CM, Leon KE, Witchley JN, Diep J, DeRisi JL.** 2016. Identification of *Plasmodium falciparum* specific translation inhibitors from the MMV Malaria Box using a high throughput in vitro translation screen. Malar J **15:**173. http://dx.doi.org/10.1186/s12936-016-1231-8.
11. **Paiardini A, Bamert RS, Kannan-Sivaraman K, Drinkwater N, Mistry SN, Scammells PJ, McGowan S.** 2015. Screening the Medicines for Malaria Venture "Malaria Box" against the *Plasmodium falciparum* aminopeptidases, M1, M17 and M18. PLoS One **10:**e0115859. http://dx.doi.org/10.1371/journal.pone.0115859.
12. **Sanders NG, Sullivan DJ, Mlambo G, Dimopoulos G, Tripathi AK.** 2014. Gametocytocidal screen identifies novel chemical classes with *Plasmodium falciparum* transmission blocking activity. PLoS One **9:**e105817. http://dx.doi.org/10.1371/journal.pone.0105817.
13. **Ruecker A, Mathias DK, Straschil U, Churcher TS, Dinglasan RR, Leroy D, Sinden RE, Delves MJ.** 2014. A male and female gametocyte functional viability assay to identify biologically relevant malaria transmission-blocking drugs. Antimicrob Agents Chemother **58:**7292–7302. http://dx.doi.org/10.1128/AAC.03666-14.
14. **Bowman JD, Merino EF, Brooks CF, Striepen B, Carlier PR, Cassera MB.** 2014. Antiapicoplast and gametocytocidal screening to identify the mechanisms of action of compounds within the Malaria Box. Antimicrob Agents Chemother **58:**811–819. http://dx.doi.org/10.1128/AAC.01500-13.
15. **Lucantoni L, Duffy S, Adjalley SH, Fidock DA, Avery VM.** 2013. Identification of MMV Malaria Box inhibitors of *Plasmodium falciparum* early-stage gametocytes using a luciferase-based high-throughput assay. Antimicrob Agents Chemother **57:**6050–6062. http://dx.doi.org/10.1128/AAC.00870-13.
16. **Duffy S, Avery VM.** 2013. Identification of inhibitors of *Plasmodium falciparum* gametocyte development. Malar J **12:**408. http://dx.doi.org/10.1186/1475-2875-12-408.
17. **Fong KY, Sandlin RD, Wright DW.** 2015. Identification of β-hematin

inhibitors in the MMV Malaria Box. Int J Parasitol Drugs Drug Resist **5:**84–91. http://dx.doi.org/10.1016/j.ijpddr.2015.05.003.
18. **Swann J, Corey V, Scherer CA, Kato N, Comer E, Maetani M, Antonova-Koch Y, Reimer C, Gagaring K, Ibanez M, Plouffe D, Zeeman AM, Kocken CH, McNamara CW, Schreiber SL, Campo B, Winzeler EA, Meister S.** 2016. High-throughput luciferase-based assay for the discovery of therapeutics that prevent malaria. ACS Infect Dis **2:**281–293. http://dx.doi.org/10.1021/acsinfecdis.5b00143.
19. **Plouffe DM, Wree M, Du AY, Meister S, Li F, Patra K, Lubar A, Okitsu SL, Flannery EL, Kato N, Tanaseichuk O, Comer E, Zhou B, Kuhen K, Zhou Y, Leroy D, Schreiber SL, Scherer CA, Vinetz J, Winzeler EA.** 2016. High-throughput assay and discovery of small molecules that interrupt malaria transmission. Cell Host Microbe **19:**114–126. http://dx.doi.org/10.1016/j.chom.2015.12.001.
20. **Hostettler I, Muller J, Hemphill A.** 2016. In vitro screening of the open source MMV Malaria Box reveals novel compounds with profound activities against *Theileria annulata* schizonts. Antimicrob Agents Chemother **60:**3301–3308. http://dx.doi.org/10.1128/AAC.02801-15.
21. **Khraiwesh M, Leed S, Roncal N, Johnson J, Sciotti R, Smith P, Read L, Paris R, Hudson T, Hickman M, Grogl M.** 2016. Antileishmanial activity of compounds derived from the medicines for malaria venture open access box against intracellular *Leishmania major* amastigotes. Am J Trop Med Hyg **94:**340–347. http://dx.doi.org/10.4269/ajtmh.15-0448.
22. **Bilsland E, Bean DM, Devaney E, Oliver SG.** 2016. Yeast-based high-throughput screens to identify novel compounds active against *Brugia malayi*. PLoS Negl Trop Dis **10:**e0004401. http://dx.doi.org/10.1371/journal.pntd.0004401.
23. **Jefferson T, McShan D, Warfield J, Ogungbe IV.** 2016. Screening and identification of inhibitors of *Trypanosoma brucei* cathepsin L with antitrypanosomal activity. Chem Biol Drug Des **87:**154–158. http://dx.doi.org/10.1111/cbdd.12628.
24. **Kaiser M, Maes L, Tadoori LP, Spangenberg T, Ioset JR.** 2015. Repurposing of the Open Access Malaria Box for kinetoplastid diseases identifies novel active scaffolds against trypanosomatids. J Biomol Screen **20:**634–645. http://dx.doi.org/10.1177/1087057115569155.
25. **Aleman Resto Y, Fernandez Robledo JA.** 2014. Identification of MMV Malaria Box inhibitors of *Perkinsus marinus* using an ATP-based bioluminescence assay. PLoS One **9:**e111051. http://dx.doi.org/10.1371/journal.pone.0111051.
26. **Njuguna JT, von Koschitzky I, Gerhardt H, Lammerhofer M, Choucry A, Pink M, Schmitz-Spahnke S, Bakheit MA, Strube C, Kaiser A.** 2014. Target evaluation of deoxyhypusine synthase from *Theileria parva* the neglected animal parasite and its relationship to Plasmodium. Bioorg Med Chem **22:**4338–4346. http://dx.doi.org/10.1016/j.bmc.2014.05.007.
27. **Boyom FF, Fokou PVT, Tchokouaha LRY, Spangenberg T, Mfopa AN, Kouipou RMT, Mbouna CJ, Donfack VFD, Zollo PHA.** 2014. Repurposing the open access malaria box to discover potent inhibitors of *Toxoplasma gondii* and *Entamoeba histolytica*. Antimicrob Agents Chemother **58:**5848–5854. http://dx.doi.org/10.1128/AAC.02541-14.
28. **Bessoff K, Spangenberg T, Foderaro JE, Jumani RS, Ward GE, Huston CD.** 2014. Identification of *Cryptosporidium parvum* active chemical series by repurposing the Open Access Malaria Box. Antimicrob Agents Chemother **58:**2731–2739. http://dx.doi.org/10.1128/AAC.02641-13.
29. **Ingram-Sieber K, Cowan N, Panic G, Vargas M, Mansour NR, Bickle QD, Wells TNC, Spangenberg T, Keiser J.** 2014. Orally active antischistosomal early leads identified from the open access malaria box. PLoS Negl Trop Dis **8:**e2610. http://dx.doi.org/10.1371/journal.pntd.0002610.
30. **Wu W, Herrera Z, Ebert D, Baska K, Cho SH, DeRisi JL, Yeh E.** 2015. A chemical rescue screen identifies a *Plasmodium falciparum* apicoplast inhibitor targeting MEP isoprenoid precursor biosynthesis. Antimicrob Agents Chemother **59:**356–364. http://dx.doi.org/10.1128/AAC.03342-14.
31. **Vos MW, Stone WJ, Koolen KM, van Gemert GJ, van Schaijk B, Leroy D, Sauerwein RW, Bousema T, Dechering KJ.** 2015. A semi-automated luminescence based standard membrane feeding assay identifies novel small molecules that inhibit transmission of malaria parasites by mosquitoes. Sci Rep **5:**18704. http://dx.doi.org/10.1038/srep18704.
32. **Lucantoni L, Silvestrini F, Signore M, Siciliano G, Eldering M, Dechering KJ, Avery VM, Alano P.** 2015. A simple and predictive phenotypic high content imaging assay for *Plasmodium falciparum* mature gametocytes to identify malaria transmission blocking compounds. Sci Rep **5:**16414. http://dx.doi.org/10.1038/srep16414.
33. **Reader J, Botha M, Theron A, Lauterbach SB, Rossouw C, Engelbrecht D, Wepener M, Smit A, Leroy D, Mancama D, Coetzer TL, Birkholtz LM.** 2015. Nowhere to hide: interrogating different metabolic parameters of *Plasmodium falciparum* gametocytes in a transmission blocking drug discovery pipeline towards malaria elimination. Malar J **14:**213. http://dx.doi.org/10.1186/s12936-015-0718-z.
34. **Sun W, Tanaka TQ, Magle CT, Huang W, Southall N, Huang R, Dehdashti SJ, McKew JC, Williamson KC, Zheng W.** 2014. Chemical signatures and new drug targets for gametocytocidal drug development. Sci Rep **4:**3743. http://dx.doi.org/10.1038/srep03743.
35. **Nam TG, McNamara CW, Bopp S, Dharia NV, Meister S, Bonamy GM, Plouffe DM, Kato N, McCormack S, Bursulaya B, Ke H, Vaidya AB, Schultz PG, Winzeler EA.** 2011. A chemical genomic analysis of decoquinate, a *Plasmodium falciparum* cytochrome b inhibitor. ACS Chem Biol **6:**1214–1222. http://dx.doi.org/10.1021/cb200105d.
36. **Rottmann M, McNamara C, Yeung BK, Lee MC, Zou B, Russell B, Seitz P, Plouffe DM, Dharia NV, Tan J, Cohen SB, Spencer KR, Gonzalez-Paez GE, Lakshminarayana SB, Goh A, Suwanarusk R, Jegla T, Schmitt EK, Beck HP, Brun R, Nosten F, Renia L, Dartois V, Keller TH, Fidock DA, Winzeler EA, Diagana TT.** 2010. Spiroindolones, a potent compound class for the treatment of malaria. Science **329:**1175–1180. http://dx.doi.org/10.1126/science.1193225.
37. **McNamara CW, Lee MC, Lim CS, Lim SH, Roland J, Nagle A, Simon O, Yeung BK, Chatterjee AK, McCormack SL, Manary MJ, Zeeman AM, Dechering KJ, Kumar TR, Henrich PP, Gagaring K, Ibanez M, Kato N, Kuhen KL, Fischli C, Rottmann M, Plouffe DM, Bursulaya B, Meister S, Rameh L, Trappe J, Haasen D, Timmerman M, Sauerwein RW, Suwanarusk R, Russell B, Renia L, Nosten F, Tully DC, Kocken CH, Glynne RJ, Bodenreider C, Fidock DA, Diagana TT, Winzeler EA.** 2013. Targeting Plasmodium PI(4)K to eliminate malaria. Nature **504:**248–253. http://dx.doi.org/10.1038/nature12782.
38. **Spillman NJ, Allen RJ, McNamara CW, Yeung BK, Winzeler EA, Diagana TT, Kirk K.** 2013. Na(+) regulation in the malaria parasite *Plasmodium falciparum* involves the cation ATPase PfATP4 and is a target of the spiroindolone antimalarials. Cell Host Microbe **13:**227–237. http://dx.doi.org/10.1016/j.chom.2012.12.006.
39. **Kuhen KL, Chatterjee AK, Rottmann M, Gagaring K, Borboa R, Buenviaje J, Chen Z, Francek C, Wu T, Nagle A, Barnes SW, Plouffe D, Lee MCS, Fidock DA, Graumans W, van de Vegte-Bolmer M, van Gemert GJ, Wirjanata G, Sebayang B, Marfurt J, Russell B, Suwanarusk R, Price RN, Nosten F, Tungtaeng A, Gettayacamin M, Sattabongkot J, Taylor J, Walker JR, Tully D, Patra KP, Flannery EL, Vinetz JM, Renia L, Sauerwein RW, Winzeler EA, Glynne RJ, Diagana TT.** 2014. KAF156 is an antimalarial clinical candidate with potential for use in prophylaxis, treatment, and prevention of disease transmission. Antimicrob Agents Chemother **58:**5060–5067. http://dx.doi.org/10.1128/AAC.02727-13.
40. **Baragaña B, Hallyburton I, Lee MCS, Norcross NR, Grimaldi R, Otto TD, Proto WR, Blagborough AM, Meister S, Wirjanata G, Ruecker A, Upton LM, Abraham TS, Almeida MJ, Pradhan A, Porzelle A, Martínez MS, Bolscher JM, Woodland A, Norval S, Zuccotto F, Thomas J, Simeons F, Stojanovski L, Osuna-Cabello M, Brock PM, Churcher TS, Sala KA, Zakutansky SE, Jiménez-Díaz MB, Sanz LM, Riley J, Basak R, Campbell M, Avery VM, Sauerwein RW, Dechering KJ, Noviyanti R, Campo B, Frearson JA, Angulo-Barturen I, Ferrer-Bazaga S, Gamo FJ, Wyatt PG, Leroy D, Siegl P, Delves MJ, Kyle DE, Wittlin S, Marfurt J, et al.** 2015. A novel multiple-stage antimalarial agent that inhibits protein synthesis. Nature **522:**315–320. http://dx.doi.org/10.1038/nature14451.
41. **Magistrado PA, Corey VC, Lukens AK, LaMonte G, Sasaki E, Meister S, Wree M, Winzeler E, Wirth DF.** 28 March 2016. *Plasmodium falciparum* cyclic amine resistance locus (PfCARL), a resistance mechanism for two distinct compound classes. ACS Infect Dis. Epub ahead of print.
42. **Flannery EL, McNamara CW, Kim SW, Kato TS, Li F, Teng CH, Gagaring K, Manary MJ, Barboa R, Meister S, Kuhen K, Vinetz JM, Chatterjee AK, Winzeler EA.** 2015. Mutations in the P-type cation-transporter ATPase 4, PfATP4, mediate resistance to both aminopyrazole and spiroindolone antimalarials. ACS Chem Biol **10:**413–420. http://dx.doi.org/10.1021/cb500616x.
43. **Flannery EL, Fidock DA, Winzeler EA.** 2013. Using genetic methods to define the targets of compounds with antimalarial activity. J Med Chem **56:**7761–7771. http://dx.doi.org/10.1021/jm400325j.
44. **Mok S, Ashley EA, Ferreira PE, Zhu L, Lin Z, Yeo T, Chotivanich K, Imwong M, Pukrittayakamee S, Dhorda M, Nguon C, Lim P, Amara-**

tunga C, Suon S, Hien TT, Htut Y, Faiz MA, Onyamboko MA, Mayxay M, Newton PN, Tripura R, Woodrow CJ, Miotto O, Kwiatkowski DP, Nosten F, Day NP, Preiser PR, White NJ, Dondorp AM, Fairhurst RM, Bozdech Z. 2015. Drug resistance. Population transcriptomics of human malaria parasites reveals the mechanism of artemisinin resistance. Science **347:**431–435. http://dx.doi.org/10.1126/science.1260403.

45. **Flannery EL, Wang T, Akbari A, Corey VC, Gunawan F, Bright AT, Abraham M, Sanchez JF, Santolalla ML, Baldeviano GC, Edgel KA, Rosales LA, Lescano AG, Bafna V, Vinetz JM, Winzeler EA.** 2015. Next-generation sequencing of patient samples shows evidence of direct evolution in drug-resistance genes. ACS Infect Dis **1:**367–379. http://dx.doi.org/10.1021/acsinfecdis.5b00049.
46. **Vincent IM, Barrett MP.** 2015. Metabolomic-based strategies for anti-parasite drug discovery. J Biomol Screen **20:**44–55. http://dx.doi.org/10.1177/1087057114551519.
47. **Patti GJ, Yanes O, Siuzdak G.** 2012. Innovation: metabolomics: the apogee of the omics trilogy. Nat Rev Mol Cell Biol **13:**263–269. http://dx.doi.org/10.1038/nrm3314.
48. **Kloehn J, Blume M, Cobbold SA, Saunders EC, Dagley MJ, McConville MJ.** 2016. Using metabolomics to dissect host-parasite interactions. Curr Opin Microbiol **32:**59–65. http://dx.doi.org/10.1016/j.mib.2016.04.019.
49. **Creek DJ, Barrett MP.** 2014. Determination of antiprotozoal drug mechanisms by metabolomics approaches. Parasitology **141:**83–92. http://dx.doi.org/10.1017/S0031182013000814.
50. **Cobbold SA, Chua HH, Nijagal B, Creek DJ, Ralph SA, McConville MJ.** 2016. Metabolic dysregulation induced in *Plasmodium falciparum* by dihydroartemisinin and other front-line antimalarial drugs. J Infect Dis **213:**276–286. http://dx.doi.org/10.1093/infdis/jiv372.
51. **Lewis IA, Wacker M, Olszewski KL, Cobbold SA, Baska KS, Tan A, Ferdig MT, Llinás M.** 2014. Metabolic QTL analysis links chloroquine resistance in *Plasmodium falciparum* to impaired hemoglobin catabolism. PLoS Genet **10:**e1004085. http://dx.doi.org/10.1371/journal.pgen.1004085.
52. **Ke H, Lewis IA, Morrisey JM, McLean KJ, Ganesan SM, Painter HJ, Mather MW, Jacobs-Lorena M, Llinas M, Vaidya AB.** 2015. Genetic investigation of tricarboxylic acid metabolism during the *Plasmodium falciparum* life cycle. Cell Rep **11:**164–174. http://dx.doi.org/10.1016/j.celrep.2015.03.011.
53. **Olszewski KL, Llinas M.** 2011. Central carbon metabolism of Plasmodium parasites. Mol Biochem Parasitol **175:**95–103. http://dx.doi.org/10.1016/j.molbiopara.2010.09.001.
54. **Olszewski KL, Morrisey JM, Wilinski D, Burns JM, Vaidya AB, Rabinowitz JD, Llinas M.** 2009. Host-parasite interactions revealed by *Plasmodium falciparum* metabolomics. Cell Host Microbe **5:**191–199. http://dx.doi.org/10.1016/j.chom.2009.01.004.
55. **MacRae JI, Dixon MW, Dearnley MK, Chua HH, Chambers JM, Kenny S, Bottova I, Tilley L, McConville MJ.** 2013. Mitochondrial metabolism of sexual and asexual blood stages of the malaria parasite *Plasmodium falciparum*. BMC Biol **11:**67. http://dx.doi.org/10.1186/1741-7007-11-67.
56. **Kelly M, Su CY, Schaber C, Crowley JR, Hsu FF, Carlson JR, Odom AR.** 2015. Malaria parasites produce volatile mosquito attractants. mBio **6:**e00235-15. http://dx.doi.org/10.1128/mBio.00235-15.
57. **Srivastava A, Creek DJ, Evans KJ, De Souza D, Schofield L, Müller S, Barrett MP, McConville MJ, Waters AP.** 2015. Host reticulocytes provide metabolic reservoirs that can be exploited by malaria parasites. PLoS Pathog **11:**e1004882. http://dx.doi.org/10.1371/journal.ppat.1004882.
58. **Ali JA, Creek DJ, Burgess K, Allison HC, Field MC, Maser P, De Koning HP.** 2013. Pyrimidine salvage in Trypanosoma brucei bloodstream forms and the trypanocidal action of halogenated pyrimidines. Mol Pharmacol **83:**439–453. http://dx.doi.org/10.1124/mol.112.082321.
59. **Trochine A, Creek DJ, Faral-Tello P, Barrett MP, Robello C.** 2014. Benznidazole biotransformation and multiple targets in Trypanosoma cruzi revealed by metabolomics. PLoS Negl Trop Dis **8:**e2844. http://dx.doi.org/10.1371/journal.pntd.0002844.
60. **Olszewski KL, Llinas M.** 2013. Extraction of hydrophilic metabolites from *Plasmodium falciparum*-infected erythrocytes for metabolomic analysis. Methods Mol Biol **923:**259–266.
61. **Fry M, Pudney M.** 1992. Site of action of the antimalarial hydroxynaphthoquinone, 2-[trans-4-(4′-chlorophenyl) cyclohexyl]-3-hydroxy-1,4-naphthoquinone (566C80). Biochem Pharmacol **43:**1545–1553. http://dx.doi.org/10.1016/0006-2952(92)90213-3.
62. **Lehane AM, Ridgway MC, Baker E, Kirk K.** 2014. Diverse chemotypes disrupt ion homeostasis in the malaria parasite. Mol Microbiol **94:**327–339. http://dx.doi.org/10.1111/mmi.12765.
63. **Spillman NJ, Kirk K.** 2015. The malaria parasite cation ATPase PfATP4 and its role in the mechanism of action of a new arsenal of antimalarial drugs. Int J Parasitol Drugs Drug Resist **5:**149–162. http://dx.doi.org/10.1016/j.ijpddr.2015.07.001.
64. **Jimenez-Diaz MB, Ebert D, Salinas Y, Pradhan A, Lehane AM, Myrand-Lapierre ME, O'Loughlin KG, Shackleford DM, Justino de Almeida M, Carrillo AK, Clark JA, Dennis AS, Diep J, Deng X, Duffy S, Endsley AN, Fedewa G, Guiguemde WA, Gomez MG, Holbrook G, Horst J, Kim CC, Liu J, Lee MC, Matheny A, Martinez MS, Miller G, Rodriguez-Alejandre A, Sanz L, Sigal M, Spillman NJ, Stein PD, Wang Z, Zhu F, Waterson D, Knapp S, Shelat A, Avery VM, Fidock DA, Gamo FJ, Charman SA, Mirsalis JC, Ma H, Ferrer S, Kirk K, Angulo-Barturen I, Kyle DE, DeRisi JL, Floyd DM, Guy RK.** 2014. (+)-SJ733, a clinical candidate for malaria that acts through ATP4 to induce rapid host-mediated clearance of *Plasmodium*. Proc Natl Acad Sci U S A **111:**E5455–62. http://dx.doi.org/10.1073/pnas.1414221111.
65. **Butterworth AS, Skinner-Adams TS, Gardiner DL, Trenholme KR.** 2013. *Plasmodium falciparum* gametocytes: with a view to a kill. Parasitology **140:**1718–1734. http://dx.doi.org/10.1017/S0031182013001236.
66. **Trager W, Jensen JB.** 1976. Human malaria parasites in continuous culture. Science **193:**673–675. http://dx.doi.org/10.1126/science.781840.
67. **Lambros C, Vanderberg JP.** 1979. Synchronization of *Plasmodium falciparum* erythrocytic stages in culture. J Parasitol **65:**418–420. http://dx.doi.org/10.2307/3280287.
68. **Cobbold SA, Vaughan AM, Lewis IA, Painter HJ, Camargo N, Perlman DH, Fishbaugher M, Healer J, Cowman AF, Kappe SH, Llinas M.** 2013. Kinetic flux profiling elucidates two independent acetyl-CoA biosynthetic pathways in *Plasmodium falciparum*. J Biol Chem **288:**36338–36350. http://dx.doi.org/10.1074/jbc.M113.503557.
69. **Kim CC, Wilson EB, DeRisi JL.** 2010. Improved methods for magnetic purification of malaria parasites and haemozoin. Malar J **9:**17. http://dx.doi.org/10.1186/1475-2875-9-17.
70. **Lu W, Clasquin MF, Melamud E, Amador-Noguez D, Caudy AA, Rabinowitz JD.** 2010. Metabolomic analysis via reversed-phase ion-pairing liquid chromatography coupled to a stand alone orbitrap mass spectrometer. Anal Chem **82:**3212–3221. http://dx.doi.org/10.1021/ac902837x.
71. **Bajad SU, Lu W, Kimball EH, Yuan J, Peterson C, Rabinowitz JD.** 2006. Separation and quantitation of water soluble cellular metabolites by hydrophilic interaction chromatography-tandem mass spectrometry. J Chromatogr A **1125:**76–88. http://dx.doi.org/10.1016/j.chroma.2006.05.019.
72. **Lu W, Kimball E, Rabinowitz JD.** 2006. A high-performance liquid chromatography-tandem mass spectrometry method for quantitation of nitrogen-containing intracellular metabolites. J Am Soc Mass Spectrom **17:**37–50. http://dx.doi.org/10.1016/j.jasms.2005.09.001.
73. **Keller A, Eng J, Zhang N, Li XJ, Aebersold R.** 2005. A uniform proteomics MS/MS analysis platform utilizing open XML file formats. Mol Syst Biol **1:**2005.0017.
74. **Clasquin MF, Melamud E, Rabinowitz JD.** 2012. LC-MS data processing with MAVEN: a metabolomic analysis and visualization engine. Current Protoc Bioinformatics Chapter **14:**Unit 14.11.
75. **Team" RC.** 2016. R: a language and environment for statistical computing. R Foundation for Statistical Computing, Vienna, Austria.
76. **Taylor SL, Ruhaak LR, Kelly K, Weiss RH, Kim K.** 19 February 2016. Effects of imputation on correlation: implications for analysis of mass spectrometry data from multiple biological matrices. Brief Bioinform. Epub ahead of print.
77. **Fang H, Gough J.** 2014. supraHex: an R/Bioconductor package for tabular omics data analysis using a supra-hexagonal map. Biochem Biophys Res Commun **443:**285–289. http://dx.doi.org/10.1016/j.bbrc.2013.11.103.
78. **Painter HJ, Morrisey JM, Mather MW, Vaidya AB.** 2007. Specific role of mitochondrial electron transport in blood-stage *Plasmodium falciparum*. Nature **446:**88–91. http://dx.doi.org/10.1038/nature05572.
79. **Srivastava IK, Rottenberg H, Vaidya AB.** 1997. Atovaquone, a broad spectrum antiparasitic drug, collapses mitochondrial membrane poten-

tial in a malarial parasite. J Biol Chem **272:**3961–3966. http://dx.doi.org/10.1074/jbc.272.7.3961.

80. **Painter HJ, Morrisey JM, Vaidya AB.** 2010. Mitochondrial electron transport inhibition and viability of intraerythrocytic *Plasmodium falciparum*. Antimicrob Agents Chemother **54:**5281–5287. http://dx.doi.org/10.1128/AAC.00937-10.
81. **Thapar MM, Gil JP, Bjorkman A.** 2005. *In vitro* recrudescence of *Plasmodium falciparum* parasites suppressed to dormant state by atovaquone alone and in combination with proguanil. Trans R Soc Trop Med Hyg **99:**62–70. http://dx.doi.org/10.1016/j.trstmh.2004.01.016.
82. **Sanz LM, Crespo B, De-Cozar C, Ding XC, Llergo JL, Burrows JN, Garcia-Bustos JF, Gamo FJ.** 2012. P. falciparum in vitro killing rates allow to discriminate between different antimalarial mode-of-action. PLoS One **7:**e30949. http://dx.doi.org/10.1371/journal.pone.0030949.
83. **Biagini GA, Fisher N, Shone AE, Mubaraki MA, Srivastava A, Hill A, Antoine T, Warman AJ, Davies J, Pidathala C, Amewu RK, Leung SC, Sharma R, Gibbons P, Hong DW, Pacorel B, Lawrenson AS, Charoensutthivarakul S, Taylor L, Berger O, Mbekeani A, Stocks PA, Nixon GL, Chadwick J, Hemingway J, Delves MJ, Sinden RE, Zeeman AM, Kocken CH, Berry NG, O'Neill PM, Ward SA.** 2012. Generation of quinolone antimalarials targeting the *Plasmodium falciparum* mitochondrial respiratory chain for the treatment and prophylaxis of malaria. Proc Natl Acad Sci U S A **109:**8298–8303. http://dx.doi.org/10.1073/pnas.1205651109.
84. **Nilsen A, LaCrue AN, White KL, Forquer IP, Cross RM, Marfurt J, Mather MW, Delves MJ, Shackleford DM, Saenz FE, Morrisey JM, Steuten J, Mutka T, Li Y, Wirjanata G, Ryan E, Duffy S, Kelly JX, Sebayang BF, Zeeman AM, Noviyanti R, Sinden RE, Kocken CH, Price RN, Avery VM, Angulo-Barturen I, Jimenez-Diaz MB, Ferrer S, Herreros E, Sanz LM, Gamo FJ, Bathurst I, Burrows JN, Siegl P, Guy RK, Winter RW, Vaidya AB, Charman SA, Kyle DE, Manetsch R, Riscoe MK.** 2013. Quinolone-3-diarylethers: a new class of antimalarial drug. Sci Transl Med **5:**177ra37. http://dx.doi.org/10.1126/scitranslmed.3005029.
85. **Baldwin J, Michnoff CH, Malmquist NA, White J, Roth MG, Rathod PK, Phillips MA.** 2005. High-throughput screening for potent and selective inhibitors of *Plasmodium falciparum* dihydroorotate dehydrogenase. J Biol Chem **280:**21847–21853. http://dx.doi.org/10.1074/jbc.M501100200.
86. **Phillips MA, Lotharius J, Marsh K, White J, Dayan A, White KL, Njoroge JW, El Mazouni F, Lao Y, Kokkonda S, Tomchick DR, Deng X, Laird T, Bhatia SN, March S, Ng CL, Fidock DA, Wittlin S, Lafuente-Monasterio M, Benito FJ, Alonso LM, Martinez MS, Jimenez-Diaz MB, Bazaga SF, Angulo-Barturen I, Haselden JN, Louttit J, Cui Y, Sridhar A, Zeeman AM, Kocken C, Sauerwein R, Dechering K, Avery VM, Duffy S, Delves M, Sinden R, Ruecker A, Wickham KS, Rochford R, Gahagen J, Iyer L, Riccio E, Mirsalis J, Bathhurst I, Rueckle T, Ding X, Campo B, Leroy D, Rogers MJ,** etal. 2015. A long-duration dihydroorotate dehydrogenase inhibitor (DSM265) for prevention and treatment of malaria. Sci Transl Med **7:**296ra111. http://dx.doi.org/10.1126/scitranslmed.aaa6645.
87. **Basco LK, Eldin de Pecoulas P, Wilson CM, Le Bras J, Mazabraud A.** 1995. Point mutations in the dihydrofolate reductase-thymidylate synthase gene and pyrimethamine and cycloguanil resistance in *Plasmodium falciparum*. Mol Biochem Parasitol **69:**135–138. http://dx.doi.org/10.1016/0166-6851(94)00207-4.
88. **Canfield CJ, Milhous WK, Ager AL, Rossan RN, Sweeney TR, Lewis NJ, Jacobus DP.** 1993. PS-15: a potent, orally active antimalarial from a new class of folic acid antagonists. Am J Trop Med Hyg **49:**121–126.
89. **Yuthavong Y, Tarnchompoo B, Vilaivan T, Chitnumsub P, Kamchonwongpaisan S, Charman SA, McLennan DN, White KL, Vivas L, Bongard E, Thongphanchang C, Taweechai S, Vanichtanankul J, Rattanajak R, Arwon U, Fantauzzi P, Yuvaniyama J, Charman WN, Matthews D.** 2012. Malarial dihydrofolate reductase as a paradigm for drug development against a resistance-compromised target. Proc Natl Acad Sci U S A **109:**16823–16828. http://dx.doi.org/10.1073/pnas.1204556109.
90. **Das S, Bhatanagar S, Morrisey JM, Daly TM, Burns JM, Jr, Coppens I, Vaidya AB.** 2016. Na+ influx induced by new antimalarials causes rapid alterations in the cholesterol content and morphology of *Plasmodium falciparum*. PLoS Pathog **12:**e1005647. http://dx.doi.org/10.1371/journal.ppat.1005647.
91. **Younis Y, Douelle F, Feng TS, Gonzalez Cabrera D, Le Manach C, Nchinda AT, Duffy S, White KL, Shackleford DM, Morizzi J, Mannila J, Katneni K, Bhamidipati R, Zabiulla KM, Joseph JT, Bashyam S, Waterson D, Witty MJ, Hardick D, Wittlin S, Avery V, Charman SA, Chibale K.** 2012. 3,5-Diaryl-2-aminopyridines as a novel class of orally active antimalarials demonstrating single dose cure in mice and clinical candidate potential. J Med Chem **55:**3479–3487. http://dx.doi.org/10.1021/jm3001373.
92. **Hameed PS, Solapure S, Patil V, Henrich PP, Magistrado PA, Bharath S, Murugan K, Viswanath P, Puttur J, Srivastava A, Bellale E, Panduga V, Shanbag G, Awasthy D, Landge S, Morayya S, Koushik K, Saralaya R, Raichurkar A, Rautela N, Roy Choudhury N, Ambady A, Nandishaiah R, Reddy J, Prabhakar KR, Menasinakai S, Rudrapatna S, Chatterji M, Jimenez-Diaz MB, Martinez MS, Sanz LM, Coburn-Flynn O, Fidock DA, Lukens AK, Wirth DF, Bandodkar B, Mukherjee K, McLaughlin RE, Waterson D, Rosenbrier-Ribeiro L, Hickling K, Balasubramanian V, Warner P, Hosagrahara V, Dudley A, Iyer PS, Narayanan S, Kavanagh S, Sambandamurthy VK.** 2015. Triaminopyrimidine is a fast-killing and long-acting antimalarial clinical candidate. Nat Commun **6:**6715. http://dx.doi.org/10.1038/ncomms7715.
93. **Juge N, Moriyama S, Miyaji T, Kawakami M, Iwai H, Fukui T, Nelson N, Omote H, Moriyama Y.** 2015. *Plasmodium falciparum* chloroquine resistance transporter is a H+-coupled polyspecific nutrient and drug exporter. Proc Natl Acad Sci U S A **112:**3356–3361. http://dx.doi.org/10.1073/pnas.1417102112.
94. **LaMonte G, Lim MY, Wree M, Reimer C, Nachon M, Corey V, Gedeck P, Plouffe D, Du A, Figueroa N, Yeung B, Bifani P, Winzeler EA.** 2016. Mutations in the *Plasmodium falciparum* cyclic amine resistance locus (PfCARL) confer multidrug resistance. mBio **7:**e00696-16. http://dx.doi.org/10.1128/mBio.00696-16.
95. **Charman SA, Arbe-Barnes S, Bathurst IC, Brun R, Campbell M, Charman WN, Chiu FCK, Chollet J, Craft JC, Creek DJ, Dong Y, Matile H, Maurer M, Morizzi J, Nguyen T, Papastogiannidis P, Scheurer C, Shackleford DM, Sriraghavan K, Stingelin L, Tang Y, Urwyler H, Wang X, White KL, Wittlin S, Zhou L, Vennerstrom JL.** 2011. Synthetic ozonide drug candidate OZ439 offers new hope for a single-dose cure of uncomplicated malaria. Proc Natl Acad Sci U S A **108:**4400–4405. http://dx.doi.org/10.1073/pnas.1015762108.
96. **Klonis N, Creek DJ, Tilley L.** 2013. Iron and heme metabolism in *Plasmodium falciparum* and the mechanism of action of artemisinins. Curr Opin Microbiol **16:**722–727. http://dx.doi.org/10.1016/j.mib.2013.07.005.
97. **Antoine T, Fisher N, Amewu R, O'Neill PM, Ward SA, Biagini GA.** 2014. Rapid kill of malaria parasites by artemisinin and semi-synthetic endoperoxides involves ROS-dependent depolarization of the membrane potential. J Antimicrob Chemother **69:**1005–1016. http://dx.doi.org/10.1093/jac/dkt486.
98. **Aroonsri A, Akinola O, Posayapisit N, Songsungthong W, Uthaipibull C, Kamchonwongpaisan S, Gbotosho GO, Yuthavong Y, Shaw PJ.** 2016. Identifying antimalarial compounds targeting dihydrofolate reductase-thymidylate synthase (DHFR-TS) by chemogenomic profiling. Int J Parasitol **46:**527–535. http://dx.doi.org/10.1016/j.ijpara.2016.04.002.
99. **Goncalves D, Hunziker P.** 2016. Transmission-blocking strategies: the roadmap from laboratory bench to the community. Malar J **15:**95. http://dx.doi.org/10.1186/s12936-016-1163-3.
100. **Birkholtz LM, Coetzer TL, Mancama D, Leroy D, Alano P.** 18 May 2016. Discovering new transmission-blocking antimalarial compounds: challenges and opportunities. Trends Parasitol. Epub ahead of print.
101. **Roncales M, Vidal-Mas J, Leroy D, Herreros E.** 2012. Comparison and optimization of different methods for the *in vitro* production of *Plasmodium falciparum* gametocytes. J Parasitol Res **2012:**927148. http://dx.doi.org/10.1155/2012/927148.
102. **D'Alessandro S, Silvestrini F, Dechering K, Corbett Y, Parapini S, Timmerman M, Galastri L, Basilico N, Sauerwein R, Alano P, Taramelli D.** 2013. A *Plasmodium falciparum* screening assay for anti-gametocyte drugs based on parasite lactate dehydrogenase detection. J Antimicrob Chemother **68:**2048–2058. http://dx.doi.org/10.1093/jac/dkt165.
103. **Peatey CL, Leroy D, Gardiner DL, Trenholme KR.** 2012. Anti-malarial drugs: how effective are they against *Plasmodium falciparum* gametocytes? Malar J **11:**34. http://dx.doi.org/10.1186/1475-2875-11-34.
104. **Fleck SL, Pudney M, Sinden RE.** 1996. The effect of atovaquone (566C80) on the maturation and viability of *Plasmodium falciparum* ga-

metocytes in vitro. Trans R Soc Trop Med Hyg **90:**309–312. http://dx.doi.org/10.1016/S0035-9203(96)90266-7.
105. **Lelievre J, Almela MJ, Lozano S, Miguel C, Franco V, Leroy D, Herreros E.** 2012. Activity of clinically relevant antimalarial drugs on *Plasmodium falciparum* mature gametocytes in an ATP bioluminescence "transmission blocking" assay. PLoS One **7:**e35019. http://dx.doi.org/10.1371/journal.pone.0035019.
106. **Bulusu V, Jayaraman V, Balaram H.** 2011. Metabolic fate of fumarate, a side product of the purine salvage pathway in the intraerythrocytic stages of *Plasmodium falciparum*. J Biol Chem **286:**9236–9245. http://dx.doi.org/10.1074/jbc.M110.173328.
107. **Plata G, Hsiao TL, Olszewski KL, Llinas M, Vitkup D.** 2010. Reconstruction and flux-balance analysis of the *Plasmodium falciparum* metabolic network. Mol Syst Biol **6:**408. http://dx.doi.org/10.1038/msb.2010.60.
108. **Liu L, Richard J, Kim S, Wojcik EJ.** 2014. Small molecule screen for candidate antimalarials targeting Plasmodium Kinesin-5. J Biol Chem **289:**16601–16614. http://dx.doi.org/10.1074/jbc.M114.551408.
109. **Vincent IM, Ehmann DE, Mills SD, Perros M, Barrett MP.** 2016. Untargeted metabolomics to ascertain antibiotic modes of action. Antimicrob Agents Chemother **60:**2281–2291. http://dx.doi.org/10.1128/AAC.02109-15.
110. **Imlay LS, Armstrong CM, Masters MC, Li T, Price KE, Edwards RL, Mann KM, Li LX, Stallings CL, Berry NG, O'Neill PM, Odom AR.** 2015. Plasmodium IspD (2-C-methyl-D-erythritol 4-phosphate cytidyltransferase), an essential and druggable antimalarial target. ACS Infect Dis **1:**157–167. http://dx.doi.org/10.1021/id500047s.
111. **Yao ZK, Krai PM, Merino EF, Simpson ME, Slebodnick C, Cassera MB, Carlier PR.** 2015. Determination of the active stereoisomer of the MEP pathway-targeting antimalarial agent MMV008138, and initial structure-activity studies. Bioorg Med Chem Lett **25:**1515–1519. http://dx.doi.org/10.1016/j.bmcl.2015.02.020.
112. **Creek DJ, Chua HH, Cobbold SA, Nijagal B, MacRae JI, Dickerman BK, Gilson PR, Ralph SA, McConville MJ.** 2016. Metabolomic-based screening of the Malaria Box reveals both novel and established mechanisms of action. Antimicrob Agents Chemother **60:**6650–6663. http://dx.doi.org/10.1128/AAC.01226-16.
113. **Howes RE, Battle KE, Satyagraha AW, Baird JK, Hay SI.** 2013. G6PD deficiency: global distribution, genetic variants and primaquine therapy. Adv Parasitol **81:**133–201. http://dx.doi.org/10.1016/B978-0-12-407826-0.00004-7.
114. **Raabe AC, Billker O, Vial HJ, Wengelnik K.** 2009. Quantitative assessment of DNA replication to monitor microgametogenesis in *Plasmodium berghei*. Mol Biochem Parasitol **168:**172–176. http://dx.doi.org/10.1016/j.molbiopara.2009.08.004.
115. **Sinden RE, Canning EU, Bray RS, Smalley ME.** 1978. Gametocyte and gamete development in *Plasmodium falciparum*. Proc R Soc Lond B Biol Sci **201:**375–399. http://dx.doi.org/10.1098/rspb.1978.0051.
116. **Canning EU, Sinden RE.** 1975. Nuclear organisation in gametocytes of Plasmodium and hepatocystis: a cytochemical study. Z Parasitenk **46:**297–299. http://dx.doi.org/10.1007/BF00418523.
117. **Peatey CL, Skinner-Adams TS, Dixon MW, McCarthy JS, Gardiner DL, Trenholme KR.** 2009. Effect of antimalarial drugs on *Plasmodium falciparum* gametocytes. J Infect Dis **200:**1518–1521. http://dx.doi.org/10.1086/644645.
118. **Goodman CD, Siregar JE, Mollard V, Vega-Rodriguez J, Syafruddin D, Matsuoka H, Matsuzaki M, Toyama T, Sturm A, Cozijnsen A, Jacobs-Lorena M, Kita K, Marzuki S, McFadden GI.** 2016. Parasites resistant to the antimalarial atovaquone fail to transmit by mosquitoes. Science **352:**349–353. http://dx.doi.org/10.1126/science.aad9279.
119. **Divo AA, Geary TG, Jensen JB.** 1985. Oxygen- and time-dependent effects of antibiotics and selected mitochondrial inhibitors on *Plasmodium falciparum* in culture. Antimicrob Agents Chemother **27:**21–27. http://dx.doi.org/10.1128/AAC.27.1.21.
120. **di Rago JP, Coppee JY, Colson AM.** 1989. Molecular basis for resistance to myxothiazol, mucidin (strobilurin A), and stigmatellin. Cytochrome b inhibitors acting at the center o of the mitochondrial ubiquinol-cytochrome c reductase in Saccharomyces cerevisiae. J Biol Chem **264:**14543–14548.
121. **Phillips MA, Gujjar R, Malmquist NA, White J, El Mazouni F, Baldwin J, Rathod PK.** 2008. Triazolopyrimidine-based dihydroorotate dehydrogenase inhibitors with potent and selective activity against the malaria parasite *Plasmodium falciparum*. J Med Chem **51:**3649–3653. http://dx.doi.org/10.1021/jm8001026.
122. **van Schalkwyk DA, Priebe W, Saliba KJ.** 2008. The inhibitory effect of 2-halo derivatives of D-glucose on glycolysis and on the proliferation of the human malaria parasite *Plasmodium falciparum*. J Pharmacol Exp Ther **327:**511–517. http://dx.doi.org/10.1124/jpet.108.141929.
123. **Vennerstrom JL, Arbe-Barnes S, Brun R, Charman SA, Chiu FC, Chollet J, Dong Y, Dorn A, Hunziker D, Matile H, McIntosh K, Padmanilayam M, Santo Tomas J, Scheurer C, Scorneaux B, Tang Y, Urwyler H, Wittlin S, Charman WN.** 2004. Identification of an antimalarial synthetic trioxolane drug development candidate. Nature **430:**900–904. http://dx.doi.org/10.1038/nature02779.
124. **Slater AF.** 1993. Chloroquine: mechanism of drug action and resistance in *Plasmodium falciparum*. Pharmacol Ther **57:**203–235. http://dx.doi.org/10.1016/0163-7258(93)90056-J.